Thesis report

Extracting and utilising heat from an hydrogen production plant

Course Code: Name

Ewoud Hermans

Delft University of Technology

TU Delft

Thesis report

Extracting and utilising heat from an hydrogen production plant

by

Ewoud Hermans

Student Name	Student Number
Ewoud Hermans	4242807

Instructor:	Ad van Wijk
Supervisor (company):	Wouter Blom
Institution:	Delft University of Technology
Place:	Faculty of Mechanical Engineering, Delft
Project Duration:	Sept, 2020 - May, 2021

Cover Image: Description + Source

TU Delft

Preface

The energy transition and the role hydrogen can play in the future sparked my interest in this topic. I would like to thank A.J.M van Wijk for giving me the opportunity to conduct my research within this field and for supervising my thesis project during this time. I would also want to thank Wouter Blom for his help, expertise and time during my thesis internship at the former Nouryon (now Nobian).

Finally, I would like to thank Ivo Pothof for finding the time to take part in the thesis committee.

Ewoud Hermans
Delft, February 2022

Abstract

In order to reach the climate goals the use of fossil fuels needs to decrease and green solution need to provide the energy of the future. Wind and solar will probably supply a large fraction of our electrical power need in the future. Because of the nature of these sources the demand for electrical power will not always be balanced with the supply. Industrial companies are responsible for a large portion of the total greenhouse emissions. Some of the emissions are process related, but most are due to the demand for high temperatures in the process. Today fossil fuels like coal and gas are used to achieve these high temperatures. Hydrogen provides a solution for the problems as it can be used as a storage medium and as an energy source to achieve high temperatures.

In order to provide the world with sufficient hydrogen needed for the transformation to greener solutions the production of hydrogen needs to increase. Hydrogen can be made from fossil fuels, but to achieve our goals the production of green hydrogen is needed. Green hydrogen is made using green electricity and the electrolysis process. In this thesis the alkaline electrolysis process is reviewed.

During the production of hydrogen using the alkaline electrolysis process, a large fraction of the electrical energy is converted to thermal energy. The aim of this research is to gain insight into the possibility of extracting the thermal energy form the process so it can be used in a district heating network.

Based on the thermal demand form the heating district and the power supply to the hydrogen plant four case studies are evaluated. Using a pinch analysis, a process flow diagram is designed for each case study after which every design is modelled. Using a heat pump and thermal storage the supply of thermal energy and the demand from the district heating network are balanced in order to reach a high overall efficiency.

Contents

List of Figures

List of Tables

1 Introduction

1.1. Context

This section will explain the context surrounding the research discussed in this report. Discussing the context will help explain the relevance of the research and provide relevant information setting the scene for hydrogen today.

1.1.1. Role of hydrogen

On the 12th of December 2015 at the COP 21 in Paris, parties of the UNFCCC reached an agreement to combat climate change. The central aim of the agreement is to keep the global temperature change well below 2 degrees Celsius compared to pre-industrial levels and to try to keep it below 1.5 degrees Celsius [26]. To achieve this target, the global CO_2 emissions must reach net-zero or very close to net zero [15]. An IRENA study in 2018 [14] shows that to bring the rise below 2 degrees Celsius by 2050, annual energy-related CO_2 emissions must decline by 70% compared with the reference case shown in figure 1.1. The reference case reflects the outcome of the current and planned policies at the moment of the study (2018). Renewable energy and energy efficiency will have to provide over 90% of the total reduction [14].

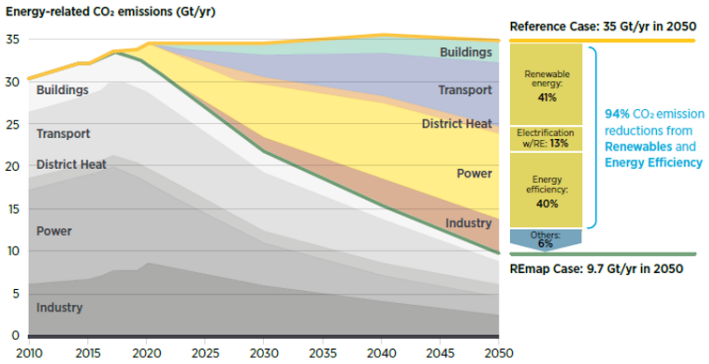

Figure 1.1: Energy related CO_2 emissions [14]

Figure 1.2 shows which contributions the different sources of energy will have in 2050 if the agreed goals are accomplished. The role of electricity will increase significantly, where most of the electricity will come from solar and wind.

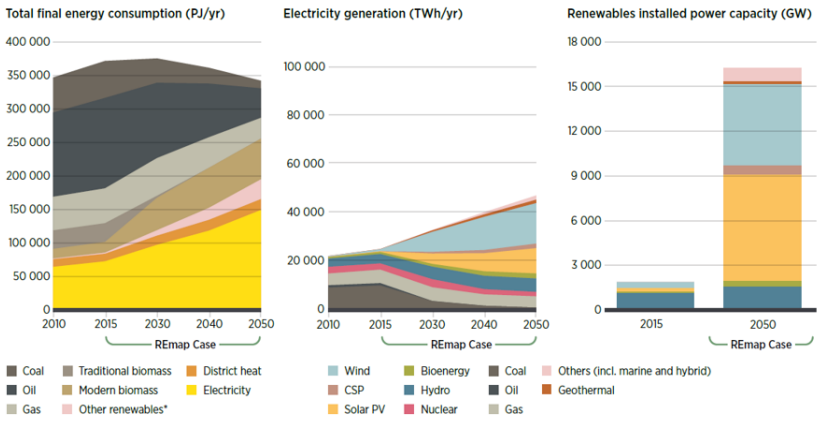

Figure 1.2: Energy consumption [14]

Hydrogen could play a mayor role in decarbonizing sectors that are difficult to electrify, such as transport, buildings and industry. Apart from being a solution to the decarbonization challenges, hydrogen could play an important role in renewable energy integration. Wind and solar are variable renewable energy sources meaning they fluctuate over time. Hydrogen could play an important role in the integration of these sources in the energy system. The large increase of these variable energy sources poses a challenge and hydrogen could be part of the solution. Because hydrogen can be stored or used in a variety of sectors, converting electricity to hydrogen can help with the matching of variable energy supply and demand, both temporally and geographically [13].

1.1.2. Hydrogen production

As of 2019, around 70 Mt of hydrogen is produced annually. The global hydrogen production accounts for 2% of the global total primary energy demand. 76% is produced from natural gas and 23% from coal. The global production of hydrogen accounts for 6% of the global natural gas use and for 2% of the global use of coal which makes it responsible for 830Mt/yr of CO_2 emissions [13].

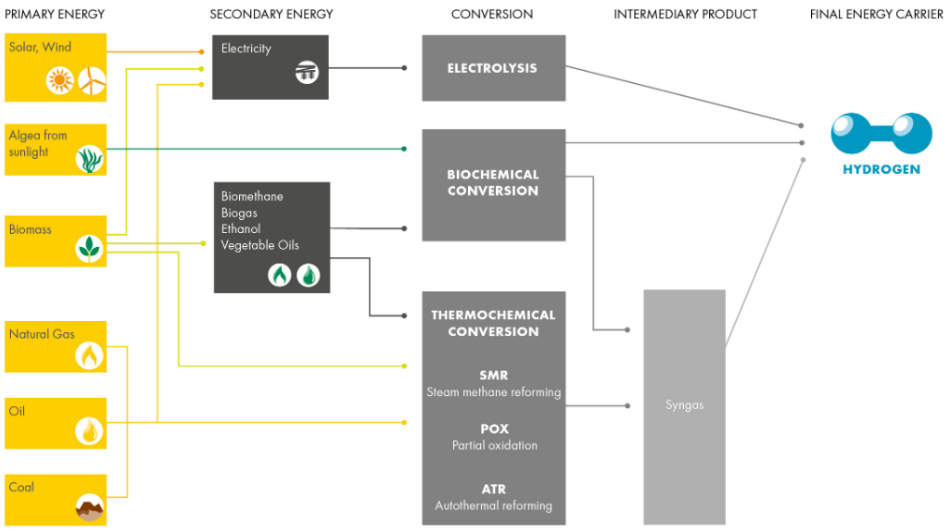

Figure 1.3: Hydrogen production methods [11]

Hydrogen is produced via multiple methods, as shown in figure 1.3. The production of hydrogen via electrolysis is the technique used for this research and will be discussed in the following chapters.

Steam reforming uses a methane source to produce hydrogen. The methane reacts under high pressures with steam to form hydrogen, carbon monoxide and carbon dioxide. A catalyst increases the

reaction. Thereafter the carbon monoxide is also converted into hydrogen and carbon dioxide in the presence of a catalyst [10].

Partial oxidation is a hydrogen production process from natural gas. The methane and other hydrocarbons in the gas react with oxygen but not enough to completely oxidize the hydrocarbons to carbon dioxide and water. The reaction products contain mostly hydrogen and carbon monoxide and just a little carbon dioxide and other reaction products. Thereafter the carbon monoxide is further reacted with water to carbon dioxide and hydrogen [10]. A combination of steam reforming and partial oxidation is called autothermal reforming where a mixture of air and water is used.

Hydrogen is also formed in industrial processes as a bi-product. Electrochemical processes, such as the industrial production of caustic soda and chlorine produce hydrogen as a waste product.

1.1.3. Problem statement

Hydrogen could play an important role in the decarbonization of the energy system of the future, since it could be the solution for decarbonizing hard to electrify sectors and help deal with the fluctuations in the generation of energy by variable renewable energy sources. Production of hydrogen will have to increase on top of the amount of hydrogen that is already produced today. With the maximum agreed temperature increase of 2 degrees Celsius in mind, the increase in hydrogen production will have to be carbon free and thus will be produced either from fossil fuels combined with carbon capture or via water electrolysis.

As figure 1.1 shows, a large part of the necessary reductions in CO_2 emissions will come from making sectors more efficient. The current cell voltage efficiency of alkaline water electrolyzers lies between 63 and 70% [13]. Cell voltage efficiency is the percentage of the total voltage applied that is used to split water into hydrogen and oxygen. Due to resistances in the electrolyzer cell, the remaining energy is converted into heat. While it is important to improve the efficiencies of alkaline water electrolyzers and reduce heat generation, it is also important to think about how we can use the technology available today in the most efficient way. The impending increase in hydrogen production and the necessity to make all sectors as efficient as possible underline the need to utilise the energy that is lost as heat in the water electrolysis process.

1.2. Nouryon

The MSc thesis presented here was carried out for the TU Delft at Nouryon. Nouryon has made a large effort to provide as much data as input for this research. Nouryon (formerly AkzoNobel Specialty Chemicals) is a company delivering essential chemicals worldwide. Nouryon is currently cooperating with partners to realise the future of hydrogen. One of their projects, the H2ermes project [2], entails the planning of a 100 MW hydrogen factory (alkaline) near Tata Steel in IJmuiden. Nouryon has many years of experience in chlor-alkali electrolysis and has been running a medium-large scale (10MW) water electrolysis plant in Norway since 1992. This thesis aims to further develop a technical understanding of the challenges in using and utilising the thermal energy generated during hydrogen production.

1.3. Objective

Large scale production of hydrogen is mostly from using fossil fuels, but with the intentions set to decrease carbon emissions large scale green hydrogen projects are popping up all over the world. The efficiency of green hydrogen production is a challenge since a percentage of the (green) electricity used is turned into heat. The objective of this study is to gain insight in the utilisation of the heat generated during the production of green hydrogen via alkaline water electrolysis. With all green hydrogen projects the business case is a problem. The costs never outweigh the benefits which means that all of the green hydrogen projects are heavily subsidised. Not only the utilisation of the generated heat will be discussed but also the economics of adding a thermal system to a water electrolysis hydrogen production project. The discussed objective leads to the main research question:

How can the heat generated in an alkaline water electrolysis plant, operated flexibly based on a wind power electricity pattern, be extracted from the process and applied in a district heating network?

Several sub questions that help answer the main research question are defined:

1. *How much thermal energy can or needs to be extracted from the process?*
2. *At what quality (temperature) can the heat extracted from the process?*
3. *What design parameters influence the quality?*
4. *What is the demand profile for the chosen application?*
5. *What is the required temperature for the chosen application?*
6. *What methods are suitable for balancing the thermal supply and demand?*
7. *What would be the cost of adding a thermal extraction and utilisation system?*

In order to gain insight into the research question, the H2ermes project is used as a case study. Based on the H2ermes project several scenarios are analysed which are discussed in section **??**. In this section the relevance of the scenarios is discussed as well. Every scenario is evaluated based on a number of criteria. The next paragraph discusses the different criteria.

1.3.1. Evaluation criteria

The following criteria are used to evaluate and compare the different scenarios:

Electrolyser efficiency (η_{elec}, %)
This is the fraction of the power from the windfarm that is used to form hydrogen and oxygen. The remaining power is converted into heat. During this research the electrolyser efficiency will not be influenced (only influenced by dependency on inputted power, but not by changing electroyser configurations), but it does show how much thermal energy will be generated. The goal should be to maximise the electrolyser efficiency. Since the efficiency is dependent on the inputted power, this evaluation criteria has to be monitored.

Fraction of generated thermal energy directly recovered ($Direct - recov - fraction$, %)
This is the fraction of thermal energy directly recovered form the total amount of heat that is generated (before addition of a heat pump). This will be in MW or in the percentage of thermal energy recovered.

Fraction of generated thermal energy recovered ($Recov - fraction$, %)
This is the total fraction of thermal energy recovered form the total amount of heat that is generated (The direcly recovered thermal energy plus the amount added by the heat pump). This will be in MW or in the percentage of thermal energy recovered. The recovered fraction should be maximised to ensure maximum overall efficiency.

Overall efficiency (η_{tot})
This is the overall efficiency of the system which is the fraction of the inputted power that is not lost (extracted thermal energy plus energy used to form oxygen and hydrogen). The inputted power is equal to the power form the windfarm plus the external power needed for the heat pump. The overall efficiency should be maximised. It is important however to look further at how much of the extracted thermal energy is actually put to use.

Fraction of normal household gas use needed ($Gas - fraction$, %)
This criteria describes the decrease in gas use for the average household within the described system. It shows the fraction of the total energy normally supplied by burning gas that still has to be supplied by using gas. This fraction should me minimised. When the value is zero, it means that all the thermal energy that was previously supplied by natural gas, is now supplied by extracted thermal energy from the hydrogen plant.

Fraction of the thermal energy recovered used ($Used - fraction$, %)
Unfortunately, supply and demand of thermal energy do not overlap. So at times when the supply is larger than the demand, thermal energy may need to be discarded when no thermal storage is added for example. This criteria describes the fraction of thermal energy recovered form the hydrogen plant

that is actually used to heat houses within the district heating network. This value should be maximised since 10% means that all the extracted thermal energy is put to use and nothing is lost.

Investment cost (C_{invest}, Euro)
The cost for adding the proposed system to the hydrogen production plant.

CO_2 avoided ($CO_2 - avoid$, m^3)
This gives the total yearly amount of CO_2 that would be avoided by adding the thermal extraction system. The CO_2 is avoided since the addition of the system reduces the amount of natural gas necessary and therefore the accompanying CO_2 emissions.

Euro invested per yearly m^3 CO_2 avoided (€/$CO_2 - avoid$, m^3)
This gives the amount of euros invested per m^3 CO_2 avoided per year. The m^3 CO_2 avoided per year is a combination of the reduction in gas use for households due to use of thermal energy from the hydrogen production plant and the used fraction. This value should be minimised. When the value becomes lower it means that per euro invested, more CO_2 is avoided.

Section 6.8 shows the values for the different criteria for every scenario so the scenarios can be compared in order to answer the research question. In section 3.7 the calculation of the different criteria is explained further.

1.4. Scope

This research focuses on the production of hydrogen using alkaline water electrolysis. Alkaline water electrolysis is the most commercially proven method due to its age and simplicity. The hydrogen plant will be assumed to be powered by a wind farm located in the North Sea. Data provided by Nouryon is used for simulating the output of such a wind farm. For the application of the extracted thermal energy this research will focus on a heating district. To simulate the demand of a heating district data provided by HVC is used. To match the demand and the supply of thermal energy from the hydrogen production plant this research will evaluate the implementation of thermal storage techniques as well as the use of a heat pump. After the technological analysis also the cost of adding thermal extraction and utilisation will be discussed.

1.5. Methodology

This section will explain how the results of the thesis research are obtained: What approach is used to come to the final conclusion, what methods are used to obtain the results and how is the research validated.

1.5.1. Methodological approach

In order to answer the main research question, the possibility of extracting and utilising thermal energy from the H2ermes project was investigated as a case study with as goal drawing more general conclusions on the feasibility of thermal energy extraction and utilisation from alkaline electrolysis hydrogen plants. The first step in the research was the analysis of the overall system and gathering all relevant data and characteristics.

The second step was to define the different constrains and goals of the overall system after which a pinch analysis will show what the most efficient design (process flow diagram) is for extracting the thermal energy at a certain quality.

The third step was the build of a model to analyse the found process flow diagram and to calculate the behaviour of the system with fluctuating power availability.

The fourth step was adding a heat pump to the model when necessary to make sure that the desired quality of thermal energy was achieved.

The fifth step was to look into the use of thermal storage to match yearly supply and demand in order to evaluate its influence on the amount of thermal energy that can be applied efficiently in a district heating system.

The final step was to do a financial analysis on the found designs in order to gain insight into the cost of adding a thermal extraction and utilisation system.

2

System description

The overall system can roughly be divided into five parts: Wind power generation, hydrogen production, thermal energy extraction, thermal balancing and application of thermal energy. In this section all parts of the system are discussed as well as their known characteristics, constrains goals and data. As mentioned, this will be done in relation to the H2ermes project. Figure 2.1 shows a schematic representation of the overall system.

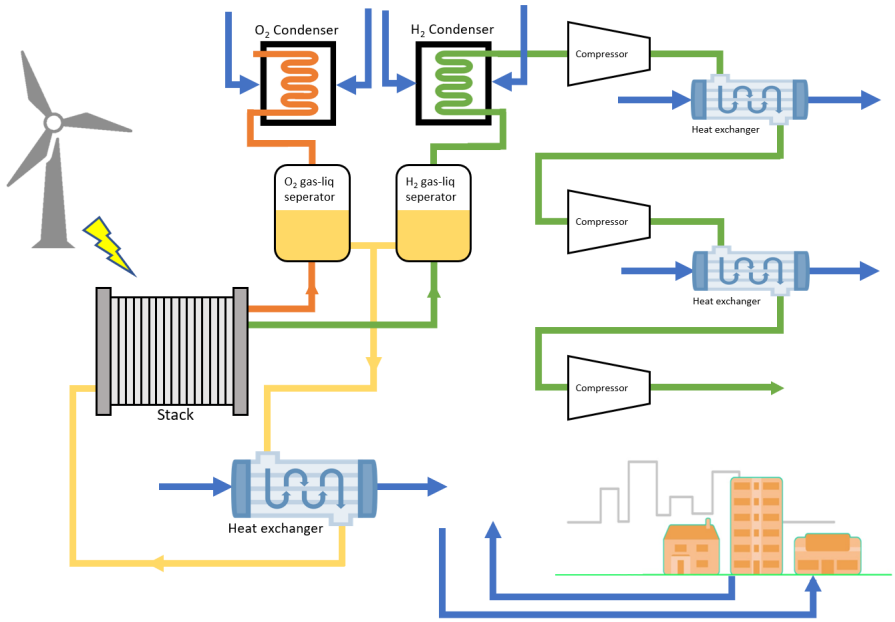

Figure 2.1: Schematic representation of the overall system

2.1. Wind power generation

For this study, the hydrogen production plant will be powered by a wind farm. As the H2ermes project is located near IJmuiden, wind power data from a wind farm maintained by Eneco in the North Sea is used. For this research it is assumed that the hydrogen production plant is directly coupled with the wind farm and that there aro o losses in therms of energy between the wind farm and the hydrogen production plant. In reality, losses in transformers, rectifiers and losses due to the distance the electricity is transported would occur. Figure 2.2 shows a graph representing the wind farm data. Since the data is confidential, the values on the axis are removed

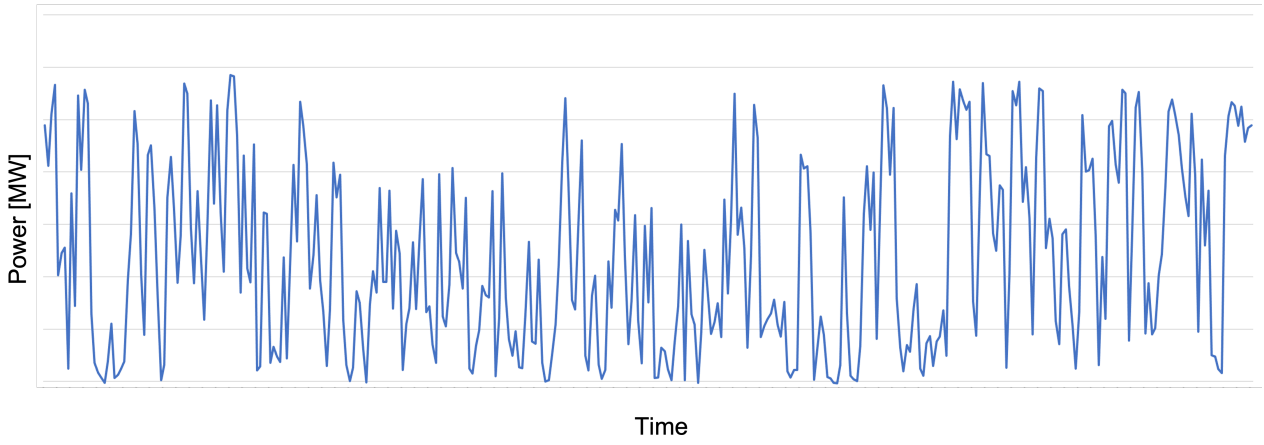

Figure 2.2: Available power form North Sea wind farm

2.2. Hydrogen production

Figure 2.3 shows a schematic of a hydrogen production plant [21]. A DC power source is connected to the electrodes of a electrolyzer stack. An electrolyzer stack is a multitude of electrolyzer cells. The schematic only shows one of these cells for simplification. There are multiple types of electrolyser cells, but for the H2ermes project alkaline electrolysers are used. The advantage of alkaline electrolyser technology is that it is more mature than other available technologies as it has been around much longer, it is cheaper than other technologies and for now, the efficiencies of large scale electrolyzers are higher [19] (see section 3 for more information).

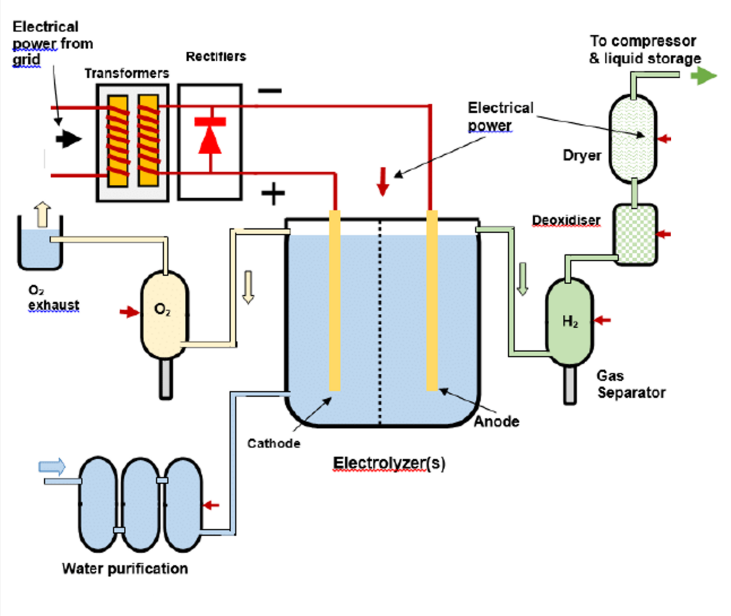

Figure 2.3: Schematic of an alkaline hydrogen production plant [21]

Each alkaline electrolyzer cell consists of two electrodes in an aqueous electrolyte solution. In the alkaline water electrolysis cell, electrons travel from the negative terminal of the DC source to the cathode where they are consumed to produce hydrogen (eq. 3.1). Hydroxide ions transfer through the electrolyte and membrane from the anode to the cathode to keep the electrical charge in balance. At the cathode they give away their electrons and water and oxygen are formed (eq. 3.2). In the case of alkaline electrolysis, the electrolyte (lye) is an alkaline solution of potassium hydroxide (KOH) or sodium hydroxide (NaOH) in water. In the case of the H2ermes project a 30 wt% KOH solution is used.

$$\text{Cathode:} \quad 2H^+ + 2e \rightarrow H_2 \tag{2.1}$$

$$\text{Anode:} \quad 2OH^- \rightarrow \frac{1}{2}O_2 + H_2O + 2e \tag{2.2}$$

Within the cells, hydrogen and oxygen are formed at the cathode and anode respectively and water is evaporated at the cathode and anode to keep up the partial pressure of water in the gaseous phase. Because of separator diaphragm between the electrodes, the hydrogen and oxygen do not mix. On the cathode sides of all the cells in the stack, the formed hydrogen and water vapor flow to a gas-liquid separator as well as liquid lye. Liquid lye is pumped through the electrolyzer stack at at constant rate to maintain the operating temperature of the stack. This is necessary because during the formation of hydrogen and oxygen due to resistances in the stack heat is formed. The gas-liquid separator is a vessel where the water vapor and hydrogen gas are separated from the liquid lye. The same process happens at the anode side for the separation of water vapor and oxygen from the liquid lye. The separated lye is cooled and pumped back into the stack, but before that extra water and some KOH is added to maintain the concentration since some water leaves in gaseous form and a little KOH leaves the separators with the gasses.

The stack is operated under a certain temperature and pressure. The temperature of the stack is determined by the manufacturer of the stack as well as the pressure and is kept constant during operation. Based on the H2ermes project, for this research a stack temperature of 80^{o}C is used and a pressure 0f 1.03 bar.

After the separation of the lye from the gaseous flows, the water vapor needs to be separated from the hydrogen and oxygen. An hydrogen and oxygen condenser condenses most of the water vapor from the hydrogen and oxygen flows respectively. The extend to how much water vapor can be removed depends on the size of the condenser and the available cooling water.

Depending on the consumer of the produced hydrogen, the hydrogen needs to be compressed to a certain pressure. In the case of the H2ermes project the pressure needs to be increased 13 times in order to meet the consumer demands.

The amount of hydrogen produced depends on the available power from the windfarm. Based on the H2ermes project a maximum production rate of 2000 kg/h of hydrogen is assumed.

2.3. Thermal energy extraction

There are four possible locations defined where heat can be extracted from the hydrogen production plant:

1. Lye cooling
2. Condensing water vapor from oxygen flow
3. Condensing water vapor from hydrogen flow
4. Cooling in between compression stages

As mentioned in the previous section, the lye separated from the gaseous flows is cooled and pumped back into the stack. For the cooling a plate heat exchanger is used. Alfalaval gives five reasons why plate heat exchangers are preferred instead of shell and tube heat exchangers. They are more efficient, use less space, are easier maintained, easier adjusted for capacity and have lower capital costs [3]. Disadvantages of plate heat exchangers are that they are that they con only be used in situations where the operating temperature is relatively low, the viscosity is low and the particulates of the products are small [8]. Since this is not the case for the purpose of this research, plate heat exchangers are preferred. The extend to which the lye needs to be cooled determines the amount of thermal energy that can be extracted at this point. The required temperature of the lye flowing into the stack depends on the amount of hydrogen that is produced at that moment, since the more hydrogen is produced, the more thermal energy is generated within the stack. An important thing to note is that it is essential that

no cooling liquid leaks into the lye stream as the impurities in the cooling medium are likely to negatively affect the energy efficiency of the electrodes in the electrolyzer.

In the oxygen and hydrogen condensers most of the water vapor is condensed from the flows by cooling. Preferably the flows are cooled as much as possible as this ensures maximum condensation. For the hydrogen condenser maximum cooling is even more important as it increases the efficiency of the compression of the hydrogen (see section 3.3.5).

To reach a pressure of 13 bar, multiple compression stages are necessary and in between stages the flow needs to be cooled as lower temperatures entering the compressor increases its efficiency. Input form Nouryon indicated that a maximum of 130^{o}C may be reached inside the compressors.

2.4. Thermal balancing

The available thermal energy extracted form the hydrogen production plant as well as the quality (temperature) of the extracted thermal energy needs to be balanced with the demand from the chosen application. The required temperature from the application as well as the amount of energy may fluctuate over time and since the hydrogen production plant is operated flexibly based on the available power from the wind farm , the available thermal energy will also fluctuate over time.

Two technologies will be used in the system to balance the supply and demand: Heat pumps and thermal storage.

Cooling of the flows will be done with cooling water from a cooling tower or air fin cooler as well as with water direct from the application.

2.4.1. Heat pump

There are a multitude of different types of heat pumps available, but for this project the vapor compression heat pump (figure 2.4) is selected with ammonia as refrigerant. The vapor compression heat pump is chosen since this technology is already proven on a large industrial scale [4] and ammonia has been widely used for heating and cooling applications, especially for large capacity energy requirements [5].

The workings of the vapor compression heat pump are as follows: A refrigerant flows though the different stages of the heat pump. In the evaporator, a heat source evaporates the refrigerant after which it is compressed by a compressor. During compression the gaseous refrigerant heats up and the pressure is increased. The high temperature high pressure vapor is condensed in the condenser where it releases latent heat which in turn can be used to heat the to be heated flow (sink). Leaving the compressor is a high pressure medium temperature liquid refrigerant which is depressurised and cooled down in the following throttling device where part of the liquid refrigerant will evaporate before reentering the evaporator [12].

The compressor power will depend on the thermal energy that needs to be added to the sink to make sure that the demand is met. Figure 2.4 shows a schematic representation of a vapor compression heat pump.

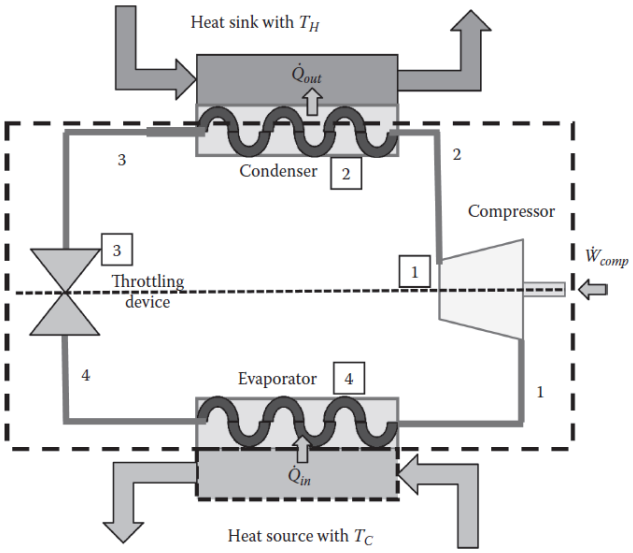

Figure 2.4: Vapor compression heat pump [4]

2.5. Application of thermal energy: District heating

District heating is an effective measure to reduce CO2 emissions (when the thermal energy is generated without the use of fossil fuels) in urban areas and hence to limit global warming. Today, the focus in district heating development is on reducing network temperatures from close to 100^{o}C to below 70^{o}C [25].

2.5.1. Thermal energy storage (TES)

Because of the increase in renewable energies, which often have a fluctuating output due to the reliance on fluctuating energy sources as solar and wind, the need to develop efficient and sustainable methods for storing energy is clear. Thermal energy storage can provide the storage of sustainable generated energy in the form of heat and resolve, for example, shortages in thermal heat due to seasonal fluctuations in solar energy. Not only can TES solve the problem between demand and supply, but it can also improve the performance, stability and thermal reliability of a system.

A first criterion is the physical phenomenon used for storing heat. From this perspective, the ongoing research focuses on three types of TES: sensible, latent and chemical storages. Sensible storages is a mature technology that have been installed in various DH networks. Latent and chemical storages are an earlier research stage; they are currently tested in experimental field installation (latent heat) or laboratory installation (thermochemical).

TES can be classified into two main families depending on the storage duration: short-term and long-term storages. In the first case the storage is used to fill the daily peak request; they have usually a duration varying from some hours to a day. Long-term TES allows storing energy for long times, from several weeks to months. They are mainly use to make available heat (or cold) stored during summer (or winter) in the season when the request is larger.

Figure 2.5 shows how various types of TES are described in the various paragraph of this section of the paper. Fig. 3 also gives an idea of the Technology Readiness Level (TRL) of the technologies, in order to show the maturity of each of the considered technologies.

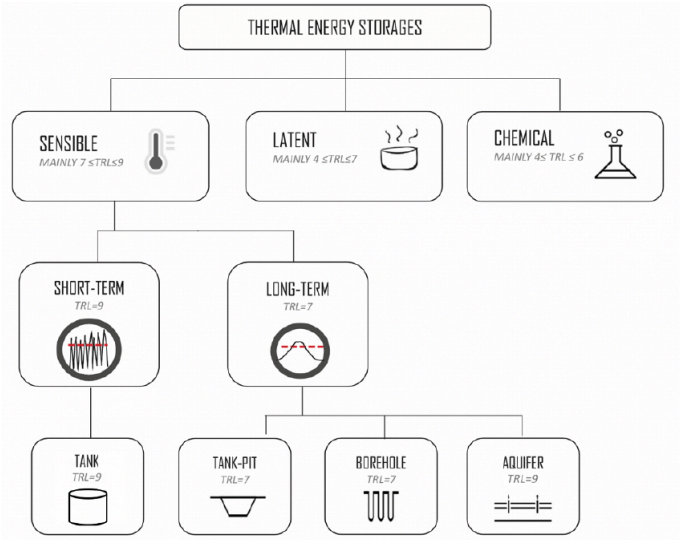

Figure 2.5: Different types of thermal storage

3

Theoretical description

3.1. Introduction

The aim of the research is to gain insight into the possibility of extracting the excess heat generated in an flexibly operated hydrogen production plant where alkaline water electrolysis is the used technology and using this heat to supply a district heating network with thermal energy. As a district heating network has a fluctuating demand, the balancing of the fluctuating supply and demand, since the plant is operated flexibly, is also within the scope of the research.

The presented research is carried out as a master thesis research at the company Nouryon. Nouryon is a company delivering essential chemicals worldwide and is currently in the process of developing multiple hydrogen production plants. One of the projects is called H2ermes where the possibility for a 100MW hydrogen factory is being investigated. This factory will be build near Tata Steel in IJmuiden. For this project Nouryon delivers the expertise and know on electrolysis, Tata steel will be the consumer and The Port of Amsterdam focuses on the infrastructure. Part of the H2ermes project is the research into the possibility of using the excess heat generated in the factory where this research done during this thesis will contribute to. This is why the H2ermes project will be used as a case study.

A modelling approach is used to gain insight into the research questions. The model will entail the total system from available power from a wind farm on the North Sea to the demand of a district near the location of the H2ermes project. The model will be the tool to asses different designs of the system and evaluate their performance over time.

The thermal output form the hydrogen plant will be modelled statically but the output will be determined for all different possible input powers. By doing this, a curve can be constructed representing the thermal output at the different locations in the system which in turn can be coupled with the output from the wind farm to obtain the results over time.

3.2. Electrolyser stack

Water electrolysis is the decomposition of water into hydrogen and oxygen in an electrochemical system (cell) composed of two electrodes, a membrane, a DC power source and an electrolyte [28]. Three main types of electrolysis cells can be classified: Alkaline, proton exchange membrane and solid oxide electrolysis cells each of which perform the same overall reaction but different half reaction occur at the electrodes. Figure 3.1 shows a schematic representation of each of the different cells.

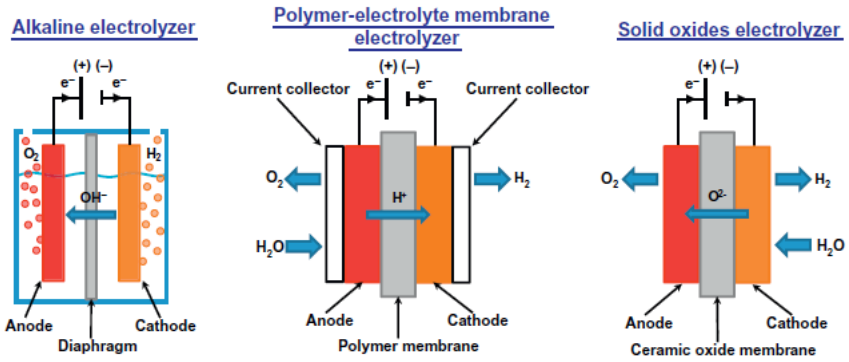

Figure 3.1: Different types of electrolysis cells [7]

In the alkaline water electrolysis cell, electrons travel from the negative terminal of the DC source to the cathode where they are consumed to produce hydrogen (eq. 3.1). Hydroxide ions transfer through the electrolyte and membrane from the anode to the cathode to keep the electrical charge in balance. At the cathode they give away their electrons and water and oxygen are formed (eq. 3.2).

$$\text{Cathode:} \quad 2H^+ + 2e \rightarrow H_2 \tag{3.1}$$

$$\text{Anode:} \quad 2OH^- \rightarrow \frac{1}{2}O_2 + H_2O + 2e \tag{3.2}$$

3.2.1. Thermodynamics of water electrolysis

The standard molar enthalpy ($\Delta_r H$) is the energy needed to split one mol of water into 0.5 mole of oxygen and 1 mole of hydrogen.

$$\Delta_r H = \Delta_r G - T\Delta_r S \tag{3.3}$$

The Gibbs free energy ($\Delta_r G$) represents the minimum electrical energy and $T\Delta_r S$ the minimum heat required for the reaction of water splitting to take place [6]. From $\Delta_r G$ the minimum required electrical energy can be calculated (reversible voltage, U_{rev}) and from $\Delta_r H$ the total electrical energy required so that no thermal energy is consumed to let the reaction take place (thermoneutral voltage, U_therm):

$$U_{rev} = \frac{\Delta_r G}{nF}\left\{ = \frac{237.22\ \text{[kJ/mol]}}{nF} = 1.23V \right\}_{stdcond} \tag{3.4}$$

$$U_{therm} = \frac{\Delta_r H}{nF}\left\{ = \frac{285.8kJ\ \text{[kJ/mol]}}{nF} = 1.48V \right\}_{stdcond} \tag{3.5}$$

Here F is the Faraday constant (96485 C/mol) and n is the number of electrons exchanged (n=2).

Figure 3.2 shows a graph of the two voltages as a function of time. When an electrolysis cell operates below the equilibrium voltage, no reaction occurs. When the cell operates between the equilibrium voltage and the thermoneutral voltage, the reaction is endothermic and will need the supply of heat. Above the thermoneutral voltage the reaction will be exothermic and heat has to be managed [6].

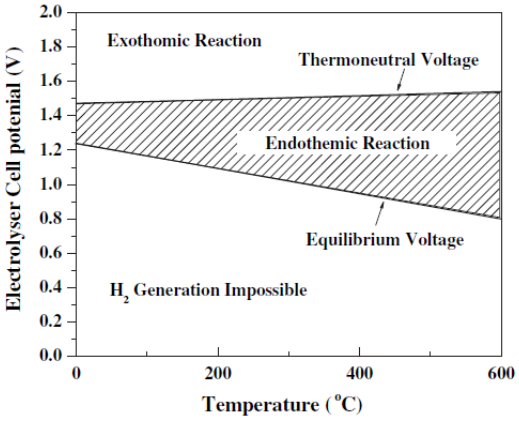

Figure 3.2: Cell potential for H_2 production as a function of temperature (standard conditions) [28]

3.2.2. Total cell potential

When modelling a alkaline water electrolysis cell the relation between the total cell voltage and the current through the cell needs to be determined. This relation is dependent on a lot of parameters. Figure 3.3 shows a plot of the relation between the current density and the total cell voltage [28].

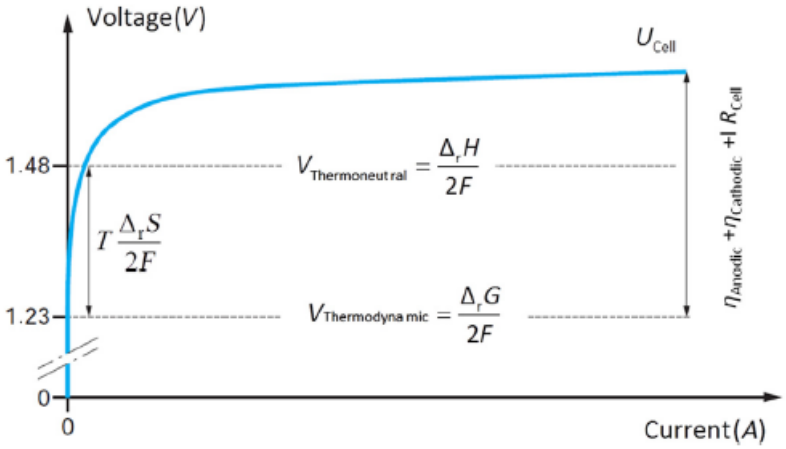

Figure 3.3: Relation between voltage and current density of electrolysis cell at 80^{o}C [28]

As figure 3.3 shows, the value of the voltage of a water electrolysis cell is dependent on a number of other potentials. The total cell voltage is calculated via:

$$U_{cell} = U^{rev} + \eta_A(i) + \eta_C(i) + iR_{cell} \tag{3.6}$$

The total voltage of an electrolysis cell directly influences the (voltage) efficiency of the cell and should always be minimised.

$$\%\text{voltage efficiency} = \frac{(E_{anode} - E_{cathode})100}{U_{cell}} \tag{3.7}$$

Where $E_{anode} - E_{cathode}$ is the equilibrium cell voltage and U_{cell} is the total voltage applied to the electrolysis cell.

For this research the electrolyser itself (the relation between the the voltage and the current density of the electrolysis cells) is not modelled. Based on expertise from Nouryon, an assumption is made for the linear part of the relation shown in figure 3.3. Assuming that during operation the hydrogen plant will never reach a current of zero, the non-linear part of the relation is neglected. In order to gain more insight into the relation, the literature was evaluated and is presented in this section.

Equilibrium cell voltage
U^{rev} is the equilibrium cell voltage or reversible voltage. This is the minimum voltage that needs to be applied. It can also be seen as the potential difference between the cathode and anode when no current is flowing. It is also referred to as the electromotive force. Equation 3.4 calculates the equilibrium cell voltage under standard conditions , but as figure 3.2 shows, U_{rev} is dependent on temperature (as well as U_{therm}). U_{rev} is calculated using the Nernst equation:

$$U^{rev} = E_{anodic} - E_{cathodic} = E^o_{an} - E^o_{ca} + \frac{RT}{nF} ln \frac{a^2_{H_2} * a_{O_2}}{a^2_{H_2O}} \tag{3.8}$$

Here $E^o_{an} - E^o_{ca}$ is the potential difference under standard condition (1.48V), R is the gas constant (R=8.314 J/(molK)), n is the number of electrons exchanged (n=4) and a_x are the activities of the chemical species. The activities can be calculated by dividing the pressure by the standard pressure (a=1 for water at standard conditions).

Oxidation and reduction overpotentials
The reaction kinetics at the electrodes are not infinite, and these limitations involves the appearance of oxidation and reduction overpotentials, $\eta_{anodic}(i)$ and $\eta_{cathodic}(i)$, respectively, leading to an over-voltage, i.e., a difference between the voltage applied to the cell during operation and the value of the reversible potential for hydrogen and oxygen production. With a simplified version of the Butler-Volmer relation the oxidation and reduction overpotentials can be calculated [7]:

$$j = j^0 \left[exp\left(\frac{\alpha nF}{RT} \eta_{anodic} \right) - exp\left(\frac{\beta nF}{RT} \eta_{cathodic} \right) \right] \tag{3.9}$$

j is the current density [A/m^2], j^0 is the exchange current density and α and β are the anodic and cathodic transfer coefficients respectively ($\alpha + \beta$=1).
In a second approximation, considering that the anodic overvoltage is large enough (e.g., in the case of water oxidation), the cathodic component becomes negligible with respect to the anodic one and the relationship becomes:

$$j = j^0 exp\left(\frac{\alpha nF}{RT} \eta_{anodic} \right) \tag{3.10}$$

For the study of an electrochemical cathodic process, if $_{cathodic}$ is large enough, then the anodic component becomes negligible. The relationship is simplified as:

$$j = -j^0 exp\left(\frac{\beta nF}{RT} \eta_{cathodic} \right) \tag{3.11}$$

From both these equations, the Tafel equations can be expressed as the over-voltages as a function of the current density:

$$\eta_{anodic} = \frac{-2.3RT}{\alpha nF} log(j^0) + \frac{2.3RT}{\alpha nF} log(j) \tag{3.12}$$

$$\eta_{cathodic} = \frac{2.3RT}{\beta nF} log(j^0) + \frac{-2.3RT}{\beta nF} log(j) \tag{3.13}$$

The exchange current density can be calculated via the following equation:

$$j^0 = \gamma_M exp\Big[- \frac{U_{rev}}{R} \Big(\frac{1}{T} - \frac{1}{T_{ref}} \Big) \Big] j^0_{ref} \tag{3.14}$$

γ_M represents the electrode roughness factor and j^o_{ref} is the reference exchange current density at T_{ref}.

Potential drop due to resistances (Ohmic losses)
Figure 3.4 shows the resistances (the barriers) presented in a typical water electrolysis system. The different resistance are classified in three groups: Electrical resistances, transport-related resistances and electrochemical reaction resistances. The electrical and transport-related resistances cause heat generation and thus inefficiency of the electrolysis system.

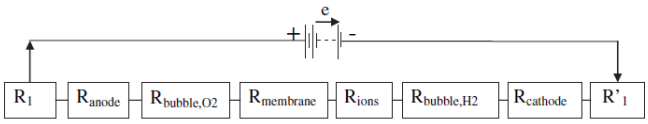

Figure 3.4: Resistances in an electrolysis cell

R_1 and R_1' are the electrical resistances in the external circuit including wiring and connections. R_{anode} and $R_{cathode}$ are electrochemical reaction resistances caused by the overpotential of oxygen and hydrogen evolution on the electrode surfaces. R_{bubble,O_2} and R_{bubble,H_2} are transport-related resistances caused by the oxygen and hydrogen bubbles formed at the electrode surfaces. These bubbles increase the path that hydroxide and hydrogen ions have to travel to arrive at the electrodes and hinder the contact between electrodes and electrolyte. The resistance added by the membrane and the electrolyte itself are denoted by $R_{membrane}$ and R_{ions} respectively [28].
The total resistance is calculated via:

$$R_{total} = R_1 + R_{anode} + R_{bubble,O_2} + R_{ions} + R_{membrane} + R_{bubble,O_2} + R_{cathode} + R_1^{'} \tag{3.15}$$

Electrode resistances The electrode resistance at any temperature is calculated via [1]:

$$R_{an} = \rho_{eff}^{an} \frac{\delta_{an}}{A_e} \quad \& \quad R_{ca} = \rho_{eff}^{ca} \frac{\delta_{ca}}{A_e} \tag{3.16}$$

Where δ is the electrode thickness, A_e the electrode surface and ρ_{eff} is the effective resistivity, which is calculated via [1]:

$$\rho_{eff}^{an} = \frac{\rho_0^{an}}{(1-\epsilon_{an})^{3/2}} \quad \& \quad \rho_{eff}^{ca} = \frac{\rho_0^{ca}}{(1-\epsilon_{ca})^{3/2}} \tag{3.17}$$

Here ρ_0 is the resistivity of a 100% dense anode/cathode material at reference temperature and ϵ is the porosity of the anode/cathode. To calculate the total electrode resistance as a function of temperature, combining equation 3.16 and 3.17 gives [1]:

$$R_e = R_{an} + R_{ca} = \frac{\rho_0^{an}}{(1-\epsilon_{an})^{3/2}} \frac{\delta_{an}}{A_e} \left[1 + \kappa_{an}\left(T - T_{ref}\right)\right] + \frac{\rho_0^{ca}}{(1-\epsilon_{ca})^{3/2}} \frac{\delta_{ca}}{A_e} \left[1 + \kappa_{ca}\left(T - T_{ref}\right)\right] \tag{3.18}$$

κ is here the temperature coefficient of resistivity.

Electrolyte resistance The electrolyte is divided into a bubble free zone (bf) and a bubble zone (bz). The length between the anode and the membrane is denoted by l_{an-s} and the length between the cathode and the membrane with l_{ca-s}. The width of the bobble zones is denoted by β_{an} and β_{ca} for the anode and cathode respectively [1].

$$R_{ions}^{an} = R_{bf}^{an} + R_{bz}^{an} = \rho_{el} \frac{l_{an-s} - \beta_{an}}{A_e} + \rho_{bz}^{an} \frac{\beta_{an}}{A_e} \tag{3.19}$$

Where ρ_{el} is the resistivity of the bubble free electrolyte and ρ_{bz}^{an} the effective resistivity in the bubble zone which can be determined via Bruggeman's model:

$$\rho_{bz}^{an} = \frac{\rho_{el}}{(1-\phi_{an})^{3/2}} \tag{3.20}$$

Where ϕ_{an} is the bubble volume fraction. The same equations can be used for the electrolyte resistance at the cathode side. The total resistance is then the sum of R_{ions}^{an} and R_{ions}^{ca}.

Membrane resistance The membrane, with as function blocking the gasses, must provide ionic conduction. Porous through the membrane provide this conduction with ϵ_s as the porosity (volume fraction of the pores). The effective length of the pores divided by the membrane thickness gives the tortuosity [1]:

$$\tau_s = \frac{l_{eff}}{\delta_s} \tag{3.21}$$

The ratio of electrolyte absorbed in the pores and the pore volume gives the wettablity factor of the membrane (ω_s). The total membrane resistance is then calculated with:

$$R_{membrane} = \rho_{el} \frac{\tau_s^2 \delta_s}{\omega_s \epsilon_s A_s} \tag{3.22}$$

3.2.3. Hydrogen & oxygen generation

The total amount of hydrogen and oxygen produced (per cell) at the cathode and anode respectively are related to the cell current via Faraday's law of electrolysis:

$$\dot{n}_{H_2} = \frac{I}{nF} = \frac{I}{2F} \quad [mol/s] \tag{3.23}$$

$$\dot{n}_{O_2} = \frac{I}{nF} = \frac{I}{4F} \quad [mol/s] \tag{3.24}$$

Here n represents the number of electrons transferred. In the case of producing one hydrogen molecule, two electrons are needed (n=2) and when producing one molecule of oxygen four electrons are released (n=4). F is the Faraday constant (96585 C/mol).

3.2.4. Thermal

When the operating voltage U_{cell} is equal to the thermoneutral voltage U_{therm}, the theoretical efficiency of an electrolyser could be 100%. No heat is needed for the reaction to occur and no heat is generated. Looking at figure 3.3, the corresponding current at the thermoneutral voltage is very low, which means that the amount of hydrogen produced will also be low as this is directly dependent on the cell current (eq. 3.23 & 3.24). At operating voltages higher than the thermoneutral voltage heat is generated in the electrolysis cells. The total amount of heat generated is the difference between the thermoneutral voltage and the operating voltage times the cell current:

$$\dot{Q}_{gen} = I * (U_{cell} - U_{therm}) \tag{3.25}$$

The generated thermal energy heat up the electrolysis cell, but since there is flow of oxygen, hydrogen and water vapor leaving the cell, part of the generated thermal energy is consumed by the evaporation of water to maintain the partial pressure of the water vapor (saturation pressure of water at cell temperature). To calculate the rate at which water evaporates in the cell the ideal gas law is used:

$$\dot{n}_{H_2} = \frac{\dot{V}}{RT} * p_{H_2} \quad \text{and} \quad \dot{n}_{H_2O} = \frac{\dot{V}}{RT} * p_{H_2O} \quad \text{result in:} \quad \dot{n}_{H_2O,cath} = \dot{n}_{H_2} * \frac{p_{H_2O}}{p_{H_2}} \tag{3.26}$$

$$\dot{n}_{O_2} = \frac{\dot{V}}{RT} * p_{O_2} \quad \text{and} \quad \dot{n}_{H_2O} = \frac{\dot{V}}{RT} * p_{H_2O} \quad \text{result in:} \quad \dot{n}_{H_2O,an} = \dot{n}_{O_2} * \frac{p_{H_2O}}{p_{O_2}} \tag{3.27}$$

Here p_{H_2O} is the partial pressure of water vapor and is equal to the saturation pressure of water at the cell temperature. From the partial pressure of water vapor the partial pressures of oxygen (p_{O_2}) and hydrogen (p_{H_2}) can be derived.

$$p_{H_2} = p_{cathode} - p_{H_2O} \quad \text{and} \quad p_{O_2} = p_{anode} - p_{H2O} \tag{3.28}$$

When assumed that the pressure on the cathode side is the same as on the anode side eq. 3.28 becomes:

$$p_{H_2} = p_{O_2} = p_{cell} - p_{H2O} \tag{3.29}$$

Subtracting the amount of heat is takes to evaporate the calculated amount of water ($\dot{n}_{H_2O,cath}$ & $\dot{n}_{H_2O,an}$) at the cathode and anode side from the total amount of heat generated ($\dot{Q}_{gen}$) gives the excess heat ($\dot{Q}_{ex}$) in the electrolysis cell. $\dot{Q}_{ex}$ is the amount of heat that needs to be removed from the cell to maintain the temperature operating temperature. The thermal energy needed for evaporation at the cathode and anode is calculated using the enthalpy of evaporation of water (ΔH_{vap}) at the cell temperature.

$$\dot{Q}_{vap,cath} = \dot{n}_{H_2O,cath} * M_{H_2O} * \Delta H_{vap} \tag{3.30}$$

$$\dot{Q}_{vap,an} = \dot{n}_{H_2O,an} * M_{H_2O} * \Delta H_{vap} \tag{3.31}$$

Here M_{H_2O} stands for the molar mass of water. The excess heat is given by:

$$\dot{Q}_{ex} = \dot{Q}_{gen} - \dot{Q}_{vap,cath} - \dot{Q}_{vap,an} \tag{3.32}$$

The energy balance an electrolysis cell. where heat loss to the environment is neglected, is given by:

$$\left[mC_p\frac{dT}{dt}\right]_{cell} = \dot{Q}_{ex} + \left[\dot{m}C_p(T_{in} - T_{out})\right]_{lye} - \left[\dot{m}C_pT\right]_{H_2O(g)} - \left[\dot{m}C_pT\right]_{H_2} - \left[\dot{m}C_pT\right]_{O_2} = 0 \tag{3.33}$$

Where $T_{lye,out}$, $T_{H_2O(g)}$, T_{H_2} and T_{O_2} are at electrolysis cell temperature. The equation is equal to zero since the cell is in steady state. As mentioned, under some operating conditions the lye flow does not need to be cooled. This happens when the amount of generated heat is smaller than the amount of thermal energy consumed by evaporating water at the anode and the cathode side. When this happens the cell cools down and the lye flow does not need to be cooled ($\dot{Q}_{ex} = 0$). The temperature of the cell can then be determined by solving the following equation:

$$\dot{Q}_{gen} = \dot{Q}_{vap,cath} + \dot{Q}_{vap,an} \tag{3.34}$$

$\dot{Q}_{vap,cath}$ and $\dot{Q}_{vap,an}$ are dependent on the partial pressure of water and the enthalpy of vaporisation of water which in turn are dependent on the cell temperature. The temperature of the cell becomes the temperature where to total amount of heat needed for evaporation is equal tot the amount of heat generated. Equation 3.34 can be rewritten as:

$$I * (U_{cell} - U_{therm}) = \dot{n}_{H_2} * \frac{p_{H_2O}}{p_{cell} - p_{H2O}} M_{H_2O}\Delta H_{vap} + \dot{n}_{O_2} * \frac{p_{H_2O}}{p_{cell} - p_{H2O}} M_{H_2O}\Delta H_{vap} \tag{3.35}$$

Rewrite eq. 3.35 so that both terms dependent on temperature are on the left side gives:

$$\Delta H_{vap} * p_{H_2O} = \frac{p_{cell} I(U_{cell} - U_{therm})}{(\dot{n}_{H_2} + \dot{n}_{O_2}) * M_{H_2O} + I(U_{cell} - U_{therm})} \tag{3.36}$$

3.3. Extraction of thermal energy

There are four possible locations defined where heat can be extracted from the hydrogen production plant:

1. Lye cooling
2. Condensing water vapor from oxygen flow
3. Condensing water vapor from hydrogen flow
4. Cooling in between compression stages

3.3.1. Heat exchanger design

As mention, plate heat exchangers/condensers will be used to transfer heat from the hot to the cold streams. In heat exchanger design the required heat exchanger area A is determined for a certain heat load Q at a given temperature gradient ΔT. The equation for calculating the required area needed for heat exchange for a certain Q and ΔT is given by:

$$A = \frac{\dot{Q}}{U \Delta T_m} \tag{3.37}$$

Here ΔT_m is the logarithmic mean temperature difference. The LMTD is a logarithmic average of the temperature difference between the hot and cold feeds at each end of the double pipe exchanger and is given by:

$$\Delta T_m = \frac{(T_H - T_C)_{in} - (T_H - T_C)_{out}}{ln[(T_H - T_C)_{in}/(T_H - T_C)_{out}]} \tag{3.38}$$

U is the overall heat-transfer coefficient and is given by:

$$U = \tag{3.39}$$

In literature [23] a range of 5000-7500 W/m^{2}K is given for plate heat exchangers that have process water on the cold and hot side and a range of 3500-4500 W/m^{2}K for plate heat exchangers with condensing stream and a process water on the hot and cold side respectively.

3.3.2. Lye cooling

As the schematic in figure 3.5 shows, two streams leaving the electrolyser stack: The stream containing the oxygen and the stream containing the hydrogen. Both streams also contain liquid lye and evaporated water. The liquid lye is separated from the gasses in the oxygen and hydrogen gas liquid separators and the excess heat ($\dot{Q}_{ex}$) is removed from the flow by an heat exchanger before it is pumped back into the electrolyser stack. This excess heat needs to be removed to maintain the operating temperature of the electrolyser stack. The temperature of the lye flow leaving the heat exchanger is given by:

$$T_{lye,out} = \frac{\dot{Q}_{ex} + \dot{m}_{lye} C_{p,lye} T_{lye,in}}{\dot{m}_{lye} C_{p,lye}} \tag{3.40}$$

3.3.3. Condensing steam from hydrogen flow

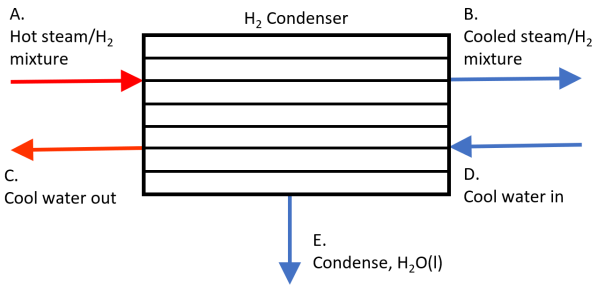

Figure 3.5: Hydrogen condenser flows

The flow leaving the hydrogen gas-liquid separator (flow A in fig. 3.5) is a mixture of steam and hydrogen at stack temperature. In the condenser the flow is cooled from the stack temperature (T_A) to a certain temperature (T_B) depending o the size of the condenser. To evaluate the amount of steam that condenses within the condenser the saturation pressure of water vapor at T_B needs to be determined. Using equation 3.26 and 3.28, the outgoing flow of steam can be determined. The total amount of thermal energy that is released during condensing is the sum of the latent heat of condensing of steam, the cooling of hydrogen, the cooling of the remaining steam and the cooling of the condensed steam.

$$\dot{Q}_{H_2,cond} = \dot{Q}_{H_2,lat} + \dot{Q}_{H_2,cool} + \dot{Q}_{steam,cool} + \dot{Q}_{water,cool} \tag{3.41}$$

The amount of latent heat released by condensing steam is given by:

$$\dot{Q}_{H_2,lat} = (\dot{m}_{H_2O(g),A} - \dot{m}_{H_2O(g),B}) * \Delta H_{vap,H_2O} \tag{3.42}$$

The amount of heat released by cooling hydrogen:

$$\dot{Q}_{H_2,cool} = \dot{m}_{H_2} C_{p,H_2} (T_A - T_B) \tag{3.43}$$

The amount of heat released by cooling steam:

$$\dot{Q}_{steam,cool} = \dot{m}_{H_2O(g),B} C_{p,H_2O(g)} (T_A - T_B) \tag{3.44}$$

The amount of heat released by cooling the condensed steam:

$$\dot{Q}_{water,cool} = (\dot{m}_{H_2O(g),A} - \dot{m}_{H_2O(g),B}) C_{p,H_2O(l)} (T_A - T_B) \tag{3.45}$$

3.3.4. Condensing steam from oxygen flow

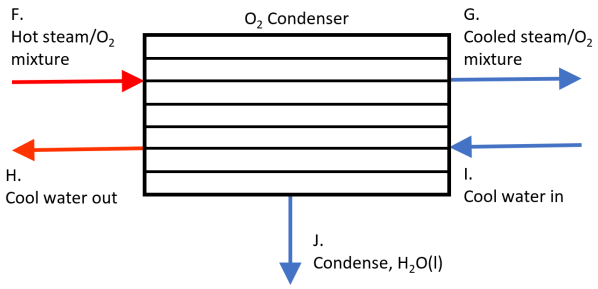

Figure 3.6: Oxygen condenser flows

The approach for calculating the amount of heat released during condensing steam from the oxygen steam mixture leaving the oxygen gas-liquid separator is the same as for the hydrogen condenser:

$$\begin{aligned} \dot{Q}_{O_2,cond} &= \dot{Q}_{O_2,lat} + \dot{Q}_{O_2,cool} + \dot{Q}_{steam,cool} + \dot{Q}_{water,cool} \\ &= (\dot{m}_{H_2O(g),F} - \dot{m}_{H_2O(g),G}) * \Delta H_{vap,H_2O} \\ &+ \dot{m}_{O_2} C_{p,O_2} (T_F - T_G) \\ &+ \dot{m}_{H_2O(g),G} C_{p,H_2O(g)} (T_F - T_G) \\ &+ (\dot{m}_{H_2O(g),F} - \dot{m}_{H_2O(g),G}) C_{p,H_2O(l)} (T_F - T_G) \end{aligned} \tag{3.46}$$

$$\dot{Q}_{cond,total} = \dot{Q}_{H_2,cond} + \dot{Q}_{O_2,cond} \tag{3.47}$$

3.3.5. Cooling between compression stages

The flow leaving the hydrogen condenser still contains a fraction of water vapor and needs to be compressed to a certain pressure for distribution to consumers (13 bar for Tata Steel in case of H2ermes). The temperature of the flow rises during compression up till a maximum allowed temperature. To reach the required pressure multiple compressors are set up in series and the flow needs to be cooled down in between the compression stages.

Although the adiabatic compression process can be assumed in centrifugal compression, polytropic compression process is commonly considered as the basis for comparing centrifugal compressor performance.

$$pV^n = constant \quad n: Polytropic\,exponent \tag{3.48}$$

The isentropic exponent k applies to the ideal frictionless adiabatic process, while the polytropic exponent n applies to the actual process with heat transfer and friction. The n is related to k through polytropic efficiency E_p:

$$\frac{n-1}{n} = \frac{k-1}{k} * \frac{1}{E_p} \tag{3.49}$$

With:

$$k = \frac{C_p}{C_v} \quad which\, gives: \; \frac{k-1}{k} = \frac{R}{C_p} \quad (R = C_p - C_v) \tag{3.50}$$

The value of C_p for the steam/hydrogen mixture is calculated via:

$$C_{p,mix} = C_{p,H_2} * x_{H_2} + C_{p,H_2O} * x_{H_2O} \tag{3.51}$$

The outgoing temperature is then calculated using the pressure ratio:

$$T_{out} = T_{in} * \left(\frac{p_{out}}{p_{in}}\right)^{\frac{R}{C_p * E_p}} \tag{3.52}$$

The required compressor power is then calculated via:

$$\dot{W}_{Comp} = \dot{m}_{Total} * C_{p,mix} * (T_{in} - T_{out}) \tag{3.53}$$

Looking at eq. 3.52, it is apparent that for high pressure ratios it is desired that the temperature of the flow entering the compressor is as low as possible since the outgoing temperature can not exceed a certain maximum value.

3.4. Thermal demand heating district

For the modelling of the thermal demand of a heating district the data obtained from HVC is used in combination with the heating degree day method and the total gas use of the to be modelled district. Thermal demand can be divided in the demand for hot water (shower etc.) and the energy needed for space heating. Both fluctuate during the day and the demand for space heating will also have a string seasonal fluctuation as it depends on the outside temperature.

3.4.1. Heating degree days

The heating degree day method assumes that no heating is necessary when the outside temperature is above a certain threshold. According to the European Environment Agency, this base value is 15.5^{o}C within Europe. A degree day is the difference between the average temperature of the day and the base value, but only when the average temperature is below the base value. When the average temperature of a certain day is 15.5^{o}C, the that day has zero degree days. In this manner the total yearly degree days can be determined. Dividing the total gas usage of a certain district by the number of degree days gives the gas per degree day of that year. This can then be used distribute the total gas use over the year to find a daily profile.

Assuming that all the gas is used for heating of water (losses for cooking neglected), the daily thermal demand of a certain district can be determined.

3.4.2. Hourly profile

The previous paragraph described how the daily thermal demand (derived form daily gas use) is obtained for a certain district. For this study it is important to obtain an hourly profile since hourly fluctuations in supply and demand will be analysed as well. In order to create the hourly profile the data set from HVC is used. From the HVC dataset an average daily profile is retrieved (figure 3.7) which then in turn is used to create the hourly profile for every day in the year in combination with the found daily profile described in the previous paragraph. By calculating the sum of a the weights shown in figure 3.7 for all 24 data points (hours) and dividing the daily thermal demand by this value you find the thermal energy per weight point of that day. This can then be used in combination with the average demand profile to find the hourly profile of that day.

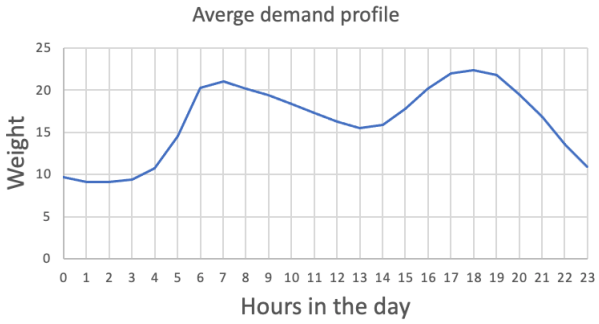

Figure 3.7: Average demand profile from HVC dataset

3.5. Balancing supply and demand

As mention, the available thermal energy needs to be balanced with the demand from the heating district. As both the demand side and supply side fluctuate over time, a technological solution needs to be found. To balance the thermal energy both a heat pump and a thermal storage system are implemented. This section describes the technologies and their theoretical background.

3.5.1. Vapor compression heat pump

Generally, vapor compression systems, which are also referred to as mechanical or refrigerative compressors have been established as the most mature machines for cooling, heat pumping and/or dehumidification purposes.

The thermodynamic cycle of vapor compression heat pumps is similar than that of the Carnot cycle. There are however some major differences. Figure 3.8 shows a schematic of a basic vapor compression heat pump. In the evaporator (4) a warm process stream evaporates a refrigerant. The refrigerant vapor is compressed (1) causing the vapor to heat up. In the condenser (2) the vapor is condensed at constant temperature and pressure as a result of heat transfer to the process stream that needs to be heated. Thereafter the liquid refrigerant passes through the throttling valve (3) and is depressurised adiabatically to return to the state before the compressor.

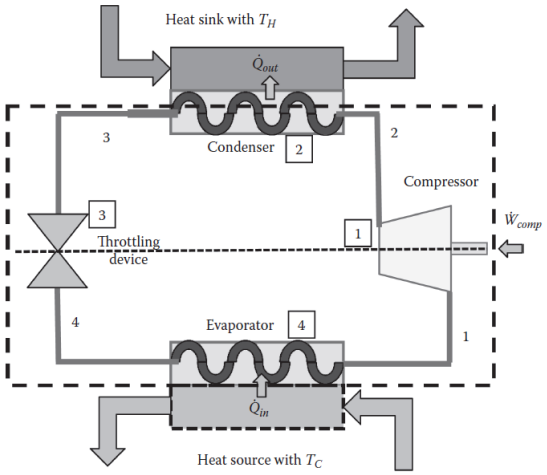

Figure 3.8: Vapor compression heat pump

In real vapor compression heat pumps this cycle differs from the Carnot cycle in the following ways:

- To reach the desired temperature of the outgoing process stream (T_H), the temperature of the refrigerant in the condenser T_2 needs to be higher since the heat transfer does not occur reversibly.

The same applies to the incoming stream T_C, which needs to be slightly higher than the desired temperature in the evaporator T_4.

- Compression in the Carnot cycle is wet. This means that a liquid-vapor mixture is compressed. Wet compression is normally avoided because the presence of liquid droplets can damage the compressor. In real vapor compression heat pumps, all of the refrigerant is evaporated, and the compression is dry. The compression process in the T-s diagram shown in figure 3.9 (process 1-2) shows that the refrigerant is compressed from a saturated vapor state (1) to a superheated saturated vapor state. This is normal for vapor compression cycles.
- Figure 3.9 also shows that the expansion process (process 2-4) does not occur along an isentropic line. The irreversible adiabatic expansion increases the entropy as there is a decrease in pressure.

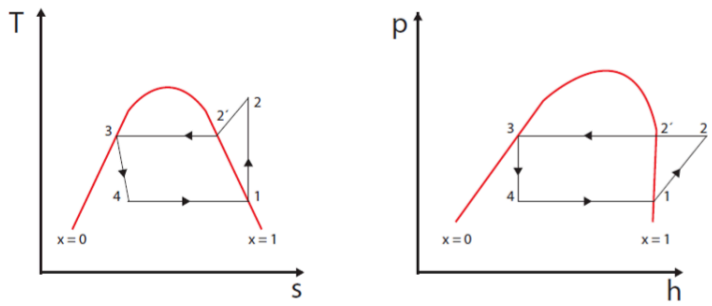

Figure 3.9: left: T-s diagram, right: p-h diagram (vapor compression cycle)

Due to differences in the real vapor compression cycle in contrast with the Carnot cycle, the COP is calculated in a different way. During the steady state operation of a vapor compression heat pump, $\dot{Q}_{in}$ and $\dot{Q}_{out}$ can be calculated via equation 3.54 where $\dot{m}$ is the mass flow rate of the refrigerant through the evaporator and condenser.

$$\dot{Q}_{in} = \dot{m}(h_2 - h1) \qquad \dot{Q}_{out} = \dot{m}(h_2 - h3) \tag{3.54}$$

Assuming no heat transfer with the environment the work done by the compressor is calculated via equation 3.55:

$$\dot{W}_{compr} = \dot{m}(h_2 - h_1) \tag{3.55}$$

The total work input into the system is the work don by the compressor. This means that the COP translates to:

$$COP = \frac{\dot{Q}_{out}}{\dot{W}_{compr}} = \frac{\dot{m}(h_2 - h3)}{\dot{m}(h_2 - h_1)} = \frac{h_2 - h_3}{h_2 - h_1} \tag{3.56}$$

It should be noted that figure 3.9 describes the ideal vapor compression cycle where irreversibilities within the condenser and evaporator are ignored, there are no frictional pressure drops, and the refrigerant flows a constant pressure through the heat exchangers. Irreversibilities in the compressor are also ignored in the ideal cycle, making it an isentropic process [16].

3.5.2. Thermal storage

Modelling the thermo-hydraulic behaviour (stratification, buoyancy, etc.) of large-scale thermal energy storage systems tends to be complex. Therefore, a wide range of tools is usually used in modelling thermal energy storage systems [9]. For the purpose of analysing the influence of adding thermal storage to the system a simplified implementation of a thermal storage system is used in this research.

It is assumed that there is no heat loss with the surroundings of the thermal (pit) storage. Assumed as well is that the hot water can be stored up until the volume of the storage is met and that the hot water is always available at the temperature at which the water was stored.

3.6. Cost estimation

This section describes how the cost for the to be added thermal extraction and application system are estimated.

3.6.1. General equipment

Adding thermal extraction and application from the electrolysis process will result in an extra investment on top of the general hydrogen production plant. Potential extra heat exchangers, piping, pumps, storage and heat pumps may have to be added. This section describes how the costs for the equipment is estimated and also the cost for installation.

A general equation for calculating the costs of equipment is given by Sinnot and Towler [24]:

$$C_e = a + b * S^n \tag{3.57}$$

Sinnot and Towler give an overview of the parameters used in the equation for a multitude of different components. This parameters for the relevant components for this study are given in table 3.1.

Equipment	Units for size, S	S lower	S upper	a	b	n
Centrifugal compressor	driver power, kW	75	5000	3800	49	0.8
Plate heat exchanger	area, m2	1.0	500	1350	180	0.95
Centrifugal pump	flow, L/s	0.2	126	6900	206	0.9
Cooling tower	flow, L/s	100	10000	150000	1300	0.9

Table 3.1: Parameters for calculating the equipment cost

Table 3.10 shows the installation factors (F) introduced by Hand (1958) which can be used to estimate the cost of equipment plus installation using equation 3.58.

$$C = F * (\sum C_e) \tag{3.58}$$

Table 6.3 Installation factors proposed by Hand (1958)

Equipment type	Installation factor
Compressors	2.5
Distillation columns	4
Fired heaters	2
Heat exchangers	3.5
Instruments	4
Miscellaneous equipment	2.5
Pressure vessels	4
Pumps	4

Figure 3.10: Installation factors for different components

The found price represents the purchased equipment cost on a U.S. Gulf Coast basis, Jan. 2007 (CE index (CEPCI). To correct for inflation the CEPCI Equipment Cost Index [18] (published monthly in Chemical Engineering) can be used in combination with the following equation:

$$Cost\ in\ year\ A = Cost\ in\ year\ B * \frac{Cost\ index\ in\ year\ A}{Cost\ index\ in\ year\ B} \tag{3.59}$$

3.6.2. Heating district piping

The CAPEX of the piping consists of both the materials costs for the piping and the installation costs. According to the Vesta MAIS model by the CE Delft [14], the CAPEX can be approached by a range of investment costs, which takes the uncertainty in installation costs due to different soils into regard. This

range is computed based on the maximal transferred heat in a section of the pipe for a temperature difference of 30 K. The range of costs is described in the Vesta MAIS model by equation 3.60 and 3.61 and gives the CAPEX in euro/meter pipe. Here, $\dot{Q_{pipe}}$ [MW] is the maximum transferred heat in the section of the pipe in regard to a temperature difference of 30 K, CAPEX$_{min}$ [e/m] is the minimal investment cost of the pipe per unit length, based on soils that are easy to excavate, such as grass or open pavement. CAPEX$_{max}$ [e/m] is the maximum investment cost of the pipe per unit length, based on soils that are difficult to excavate, such as asphalt.

$$CAPEX_{min} = 400 + 210 * max(\dot{Q}_{pipe})^{0.5} \tag{3.60}$$

$$CAPEX_{max} = 800 + 200 * max(\dot{Q}_{pipe})^{0.6} \tag{3.61}$$

3.6.3. Thermal storage

The estimated cost of the thermal energy systems considers storage material, operation costs, and technical equipment for charging and discharging the storage device. Sensible storage is rather inexpensive technology and the cost of it decreases as the size of the storage media (mostly water) increases. An important element of the system is the insulation, and it might be a significant part of the cost.

According to Schmidt [27], the aim of the development of pit storages in Denmark is to bring down the investment cost per m3 water below 35 €/m3. Most storage systems shown in figure 3.11 consist of a 5,000-10,000 m³ water container with energy content between 70-90 kWh/m³ and investment costs between 50-200 €/m³ of water equivalent. This represents specific investment cost from 0.5-3.0 €/kWh.

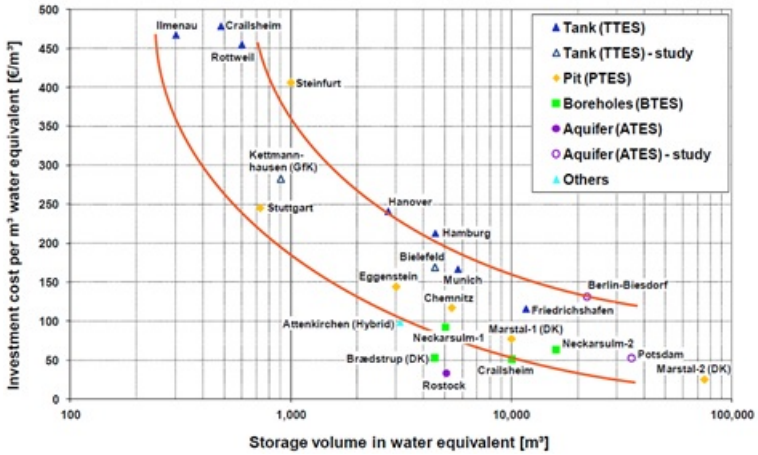

Figure 3.11: Cost for different types of thermal storage [22]

3.6.4. Heat pump

The heat pump investment costs for the investigated HP projects for different thermal capacity can be found in 3.12.

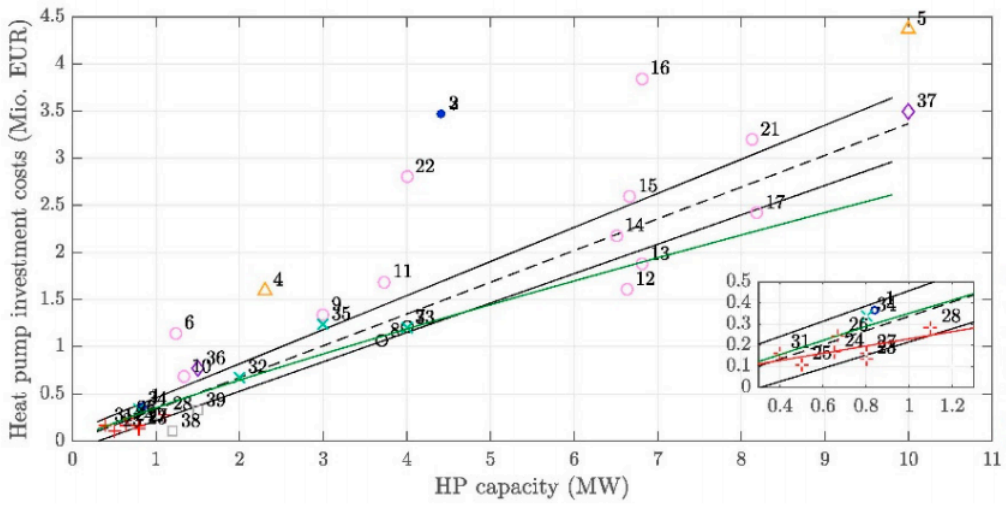

Figure 3.12: Cost heat pump [20]

3.7. Evaluation criteria definitions

This section describes how the different criteria are calculated.

3.7.1. Electrolyser efficiency

The electroyser efficiency (η_{elec}) describes the percentage of the power from the windfarm ($P_{windfarm}$, MW) that is actually used for the formation of hydrogen and oxygen. The remaining fraction is converted into heat ($\dot{Q}_{gen}$ in MW, see equation 3.25).

$$\eta_{elec} = \frac{P_{windfarm}}{\dot{Q}_{gen}} \tag{3.62}$$

3.7.2. Thermal energy directly recovered

$Direct - recov - fraction$ gives the percentage of the total generated thermal energy that is directly recovered without the use of a heat pump.

3.7.3. Total thermal energy recovered

The fraction of the thermal energy recovered ($Recov - fraction$) is calculated by subtracting the total amount of thermal energy recovered ($\dot{Q}_{recov}$, MW) from the total amount of thermal energy generated and dividing this with the total amount of thermal energy generated.

$$Recov - fraction = \frac{\dot{Q}_{recov}}{\dot{Q}_{gen}} \tag{3.63}$$

The calculation of $\dot{Q}_{recov}$ depends on the design of the system. In the results will discussed how this value is calculated based on the different designs.

3.7.4. External power needed

The external power needed (P_{ext}, MW) is the power needed to drive the compressor in case a heat pump is added to the system. To calculate P_{ext} equation 3.55 is used. Here h_1 (kJ/kg) is the enthalpy of the enthapy if the refrigerant before compression and h_1 the enthalpy after compression.

3.7.5. Overall efficiency

The overall efficiency (η_{tot}) is the efficiency of the system when it is assumed that all extracted thermal energy is actually used. It is calculated by dividing the total energy input by the sum of the energy used for the formation of hydrogen and oxygen and the thermal energy recovered.

$$\eta_{tot} = \frac{(P_{windfarm} - \dot{Q}_{gen}) + \dot{Q}_{recov}}{P_{windfarm} + P_{ext}} \tag{3.64}$$

3.7.6. Fraction of normal household gas use needed

The fraction of normal household gas use needed ($Gas - fraction$) is calculated using the average yearly gas use of a dutch household (1239 m^3). By calculating the yearly gas use after using the thermal energy extracted from the hydrogen plant and dividing this with the average yearly household gas use the fraction is calculated.

3.7.7. Fraction of the thermal energy recovered used

By adding thermal storage to the system thermal energy can be stored when the supply is high. When no thermal energy can be stored the extracted energy needs to be used immediately or otherwise discarded. This means that only a fraction of the extracted thermal energy is used. This criteria shows what that fraction is for the different scenarios.

The value is calculated by subtraction the amount of energy from gas (per year) still necessary after adding the thermal system from the total yearly demand and dividing this value by the total yearly supply.

3.7.8. CO_2 avoided

The CO_2 emission factor for natural gas is: 0.056 kg $CO_{2,eq}$/MJ energy equivalent. Since the higher heating value of natural Gas is between 38 - 39 MJ/m^3, the CO_2 emission factor would be about 2.2 kg $CO_{2,eq}$ per m^3 of natural gas. Together with the yearly average amount of natural gas per household used (1239 m^3) and $Gas - fraction$ the $CO_2 - avoid$ can be calculated. To calculate the yearly amount of kilograms avoided the following equation us use:

$$CO_2 - avoid = 2.2 * 1239 * \#Houses * (100 - Gas - fraction) \tag{3.65}$$

3.7.9. Euro invested per kilogram of CO_2 avoided

€/$CO_2 - avoid$ gives the amount of euros invested per kilogram of CO_2 avoided per year. It is calculated by dividing $CO_2 - avoid$ by C_{invest}.

3.8. Assumptions

This section gives a overview of the assumptions that where made during the research:

- The power generated by the windfarm is directly used in the electrolysers without conversion or other losses.
- Based on input from the H2ermes project, it is assumed that the maximum production capacity of the hydrogen plant is 2000 kg/h.
- The assumption is made that the pressure at the anode side of the electroyser is the same as on the cathode side. It is also assumed that the pressure within the system up to the first compressor is constant (1.03 bar). This means that pressure drops due to heat exchangers, piping and other factors are neglected.
- Within the compressors, polytopic compression is assumed.
- Within the system it is assumed that there are no heat losses with the surroundings (perfectly insulated). This is also assumed for the thermal storage so that water stored at 85^{o}C is still at that temperature when retrieved from the thermal storage.
- It is assumed that the cell voltage of the electroyser increases with 0.2 volt over 8 year (end of life).
- It is assumed that the results based on the used wind pattern give a relevant result for the future.
- It is assumed that the hydrogen plant will always be able to run and therefore deliver thermal energy.

- For the heat pump, an isentropic process is assumed in the compressor and it is assumed that there is no heat exchange with the environment.
- It is assumed that the thermal demand for the to be evaluated district can be estimated from a derivation of the data from a certain district somewhere in the Netherlands. Also, it is assumed that the demand for a district of a certain size can be calculated by multiplying the demand from the known district with a certain factor.

4

Case Study: H_2ermes

In this chapter, the different aspects of the case study will be elaborated. H2ermes is the consortium name with which since October 2018, 3 parties investigate the possibility to build a 100 MW electrolyser on the premises of Tata Steel near IJmuiden. Besides Tata Steel, the two other participants are Nouryon and Port of Amsterdam.

4.1. Velsen-Noord

For this case study the district Velsen-Noord is chosen as a potential consumer of the extracted thermal energy. Figure 4.1 shows the location of the hydrogen production plant, the roughly drawn thermal pipe that needs to be installed and the location of the thermal district. The length of the presented thermal pipe is estimated at 3 km. For the total length this value needs to be doubled as there needs to be a pipe for the hot and cold district heating water.

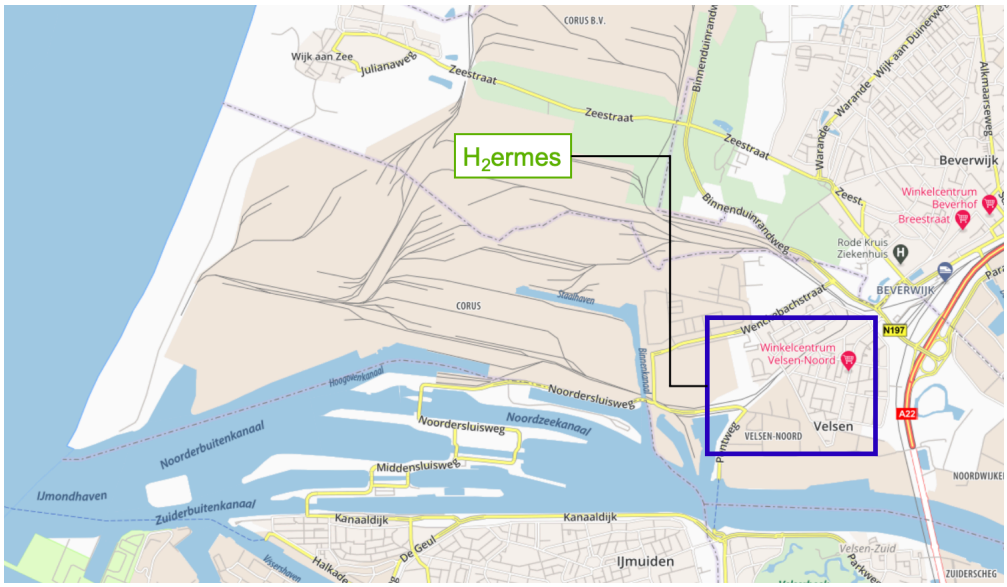

Figure 4.1: Location of plant and district

In Velsen-Noord there are a total of 2372 of residential houses and the yearly gas use in 2017 was 2560000 m^3 which gives a yearly gas use of 1079 m^3 per house. The total degree days in 2017 was 2565 which gives 997 m^3 per degree day.

4.2. Scenarios

For this study, four different scenarios were investigated, but every scenario is analysed for when the plant is at the start of life, middle of life and and of life as well as for different sizes of heating district and thermal storage. The scenarios are reviewed based on the proposed evaluation criteria discussed in section 1.3.1.

4.2.1. Scenario 1.

Scenario 1. analyses a system where the thermal demand temperature from the heating district is 85^{o}C and the electrolyser operates at a temperature of 80^{o}C. This scenario is of importance since it will show how the system can operate when the demand temperature from the heating district is higher than the temperature in the electrolysers. Older heating district networks tend to have a higher demand temperature than the newer versions and the electrolyser temperature is a design parameter given by Nouryon. This results in the fact that a heat pump is needed to achieve the demanded temperature. In this scenario it is assumed that the hydrogen factory follows the output of the wind farm entirely.

4.2.2. Scenario 2.

Scenario 2 analyses the same system as for scenario 1. The difference in this scenario is that the plant always operates at a base load of 70% of the full capacity. The remaining 30% fluctuates as a function of the available power from the wind farm. So when the wind farm has maximum output, the plant operates at 100 MW and when there is no wind the plant will operate at 70 MW. Since Tata Steel probably needs a certain amount of hydrogen, the plant will probably operate under a certain baseload. Otherwise not enough hydrogen is produced. This scenario will gain some insight on the influence of such a baseload on the discussed evaluation criteria.

4.2.3. Scenario 3.

Scenario 3. analyses a system where the thermal demand temperature from the heating district is 70^{o}C and the electrolyser operates at a temperature of 80^{o}C. Scenario 3 will help to understand what happens when the demand temperature is lower than that of the electrolyser. Newer district heating networks can have lower demand temperatures. Since a district heating network is yet to be build in and around Velsen-Noord, the demand temperature will probably be low. This makes scenario 3 a relevant case in order to investigate the feasibility of extracting and utilising the generated thermal energy. In this scenario it is assumed that the hydrogen factory follows the output of the wind farm entirely.

4.2.4. Scenario 4.

Scenario 4 analyses the same system as for scenario 3. The difference in this scenario is that the plant always operates at a base load of 70% of the full capacity. The remaining 30% fluctuates as a function of the available power from the wind farm. So when the wind farm has maximum output, the plant operates at 100 MW and when there is no wind the plant will operate at 70 MW. Since Tata Steel probably needs a certain amount of hydrogen, the plant will probably operate under a certain baseload. Otherwise not enough hydrogen is produced. This scenario will gain some insight on the influence of such a baseload on the discussed evaluation criteria.

5

Pinch analysis

5.1. Introduction

An industrial process is usually a complex system consisting of different units, for example, reactors, separators, heat exchangers, and boilers which are connected to each other and interact during operation. Analyzing such a system in order to reduce energy use is complicated, and consequently, systematic methods are needed. Process integration consists of several methods that have been developed for this purpose, focusing on system solutions of processes and interaction between different sub processes. Process integration, according to IEA's definition is: "Systematic and general methods for designing integrated production systems, ranging from individual processes to total sites, with special emphasis on the efficient use of energy and reducing environmental effects" (Gundersen, 2000).

Three methods are usually included in process integration: pinch analysis, mathematical programming (optimization), and exergy analysis. Pinch analysis is a systematic tool for investigating the possibilities of heat integration (process integration) between processes (Linnhoff et al., 1982) and is most common of the three process integration tools. In a pinch analysis, streams that need to be heated are coupled to streams that need to be cooled. Between these streams, heat exchangers are inserted, which forms a heat exchanger network of different streams. With pinch analysis, it is possible to calculate the theoretically minimum possible external heat requirement for a heat exchanger network (i.e., the amount of heat that must be added to the system via, e.g., external boilers/heat pumps) and the amount of heat that must be cooled off in the network (i.e., the amount of heat that must be cooled off in the system via, e.g., cooling towers). It is also possible to determine the amount of heat that can be exchanged internally. Different curves are developed from which the system can be analysed in different ways. From the composite curve diagram (CC), minimum possible external heating and cooling requirements, theoretically, are obtained. The same information is available from so-called grand composite curves (GCC) and in GCC foreground and background analyses can be made to identify possible integration of processes in an existing system.

This chapter will explain the concept of pinch analysis and at the same time perform the pinch analysis on the hydrogen production plant. The pinch analysis will be used to find the most efficient way of heating the water from the heating district to the required temperature. It will shows the amount of heat that directly can be transferred between streams and the external heating and cooling necessary to reach the required temperatures. The pinch analysis will be performed for the situation where the hydrogen production plant is operating at 100% capacity. This is because later on the the design process the heat exchanger sizes need to be determined and they need to be able to deliver sufficient cooling under these conditions.

5.2. Pinch analysis concept

Any flow which requires heating or cooling, but does not change in composition, is defined as a stream. The flow(s) that needs to be heated up are called cold streams and the flow(s) that need to be cooled

down are called hot streams. A reaction process is not a stream, because it involves a change in chemical composition.

The pinch analysis starts by defining all the hot and cold streams and displaying them in a table with their initial (supply, T_s) temperature and their final (target, T_t) temperature. From the mass flow rate and the specific heat capacity the heat capacity flow rate (CP) can be calculated per stream as well as the heat content H (kW) of every stream. The heat content is the thermal energy that needs to be added or removed from the cold or hot stream respectively. Equation 5.1 shows the relation between the CP and H. The CP value is assumed constant in pinch analysis.

$$Q = \int_{T_S}^{T_T} C_p \dot{m}\, dT = \int_{T_S}^{T_T} CP\, dT = CP(T_S - T_T) = \Delta H \tag{5.1}$$

A helpful method of visualisation of the flows is the temperature–heat content (T/H) diagram with in the x-axis the heat content and on the y-axis the temperature. All the steams can be represented in such a diagram where the slope of the line is given by:

$$\frac{dT}{dQ} = \frac{1}{CP} \tag{5.2}$$

The T/H diagram can be used to represent heat exchange, because of a very useful feature. Namely, since we are only interested in heat content changes of streams, a given stream can be plotted anywhere on the enthalpy axis. Provided it has the same slope and runs between the same supply and target temperatures, then wherever it is drawn on the H-axis, it represents the same stream.

As mentioned, a first step in visualising the different streams in a T/H diagram, it is essential to gather all the available data of all the streams and represent them in a data table. For the hydrogen production plant we will start with analysing the hot streams. This is because the amount of energy available will determine the flow of the cold stream (flow from heating district). Based on the found available thermal energy the flow rate will be chosen, this will be explained later.

Within the hydrogen production plant five different hot streams can be defined:

1. Stream from gas-liquid separators to stack
2. Stream from hydrogen gas-liquid separator to first compressor
3. Stream from first to second compressor
4. Stream from second to third compressor
5. (Stream from third compressor to consumer)
6. (Stream from oxygen gas-liquid separator to environment)

Stream number 1. needs to be cooled down from 80^{o}C to 58.88^{o}C (eq. 3.40) when the plant operates at full capacity (2000 kg/h of hydrogen production). The total duty for cooling stream 1. is given by eq. 3.32 and is equal to: 15 MW

Stream number 2. needs to be cooled down from 80^{o}C to 30^{o}C. The problem with this stream is that the CP value in reality is not constant due to the fact that it is a mixture of both hydrogen and water vapor. This means that during the cooling down a part of the water vapor will condense and release energy. For the purpose if designing a efficient process flow diagram using pinch analysis for now the CP will be assumed to be constant but this will later on be taken into consideration. The total duty that is necessary for cooling the flow down is given by eq. 3.41 and is equal to 10.56 MW.

Stream number 3. needs to be cooled down from 130^{o}C to 30^{o}C. For a more realistic pinch analysis this stream is segmented into two flows. Namely, constant CP cooling of the hydrogen and water vapor in the super heated region up until the dew point (sensible heat) of water (stream 3.1) and the the cooling of the stream after the dew point (stream 3.2) when condensation starts taking place (sensible and latent heat). The dew point is dependent on the partial pressure of water at this stage and is equal to 48.66^{o}C.

Stream 3.1 is the cooling of hydrogen gas and water vapor up until the dew point. This is from 130^{o}C to 48.66^{o}C. The total duty necessary for cooling this stream is equal to 0.70 MW.

Stream 3.2 is the cooling of hydrogen gas and water vapor up until the dew point. This is from 48.66^{o}C to 30^{o}C. The total duty necessary for cooling this stream is equal to 0.50 MW.

Stream number 4. is calculated in the same way as stream number 3. The results are represented in table 5.1.

Stream number 4. is calculated in the same way as stream number 3 and 4. The results are represented in table 5.1.

Because the target pressure is 13 bar and this is already accomplished before the gas mixture reaches 130^{o}C, this flow only is cooled down from 92^{o}C to 30^{o}C. Another thing to note is that the cooling down is not necessary because another compression step follows. It will be the consumer that determines the required hydrogen (water vapor) temperature, but for now 30^{o}C is assumed.

All the stream data is represented in table 5.1 and every stream can be visualised in a T/H diagram.

Stream	Hot/Cold	T_S [C]	T_T [C]	Duty [MW]	CP [MW/C]
1	Hot	80	58.88	15.07	0.71
2	Hot	80	30	10.56	0.21
3.1	Hot	130	48.66	0.70	0.094
3.2	Hot	48.66	30	0.50	0.0086
4.1	Hot	130	48.07	0.69	0.027
4.1	Hot	48.07	30	0.28	0.0084
5.1	Hot	89.96	41.77	0.40	0.0084
5.2	Hot	41.77	30	0.14	0.0119
6	Hot	80	30	4.69	0.094

Table 5.1: Stream data

From the separate streams in the T/H diagram the composite curves can be formed. The composite curves are the accumulated contents of all streams, hot or cold, available in a temperature interval between the extreme supply and targets temperatures. The formula to construct the composite curves, where the CP_j's are the active CP's in temperature interval ΔT_i and the value of H_0 can be used to shift the composite curve around, is as follows:

$$H = H_0 + \sum_j \left[\sum_j CP_j \right]_{i-1}^{i} \Delta T_i \tag{5.3}$$

For example: For the hot composite curve, the first interval is from 130^{o}C to 89.96^{o}C, so ΔT_i is equal to 40.04^{o}C. The sum of the CP's in this interval is equal to: 0.094+0.027=0.121 (from stream 3.1 and 4.1), which gives a H of 4.84 MW. The found ΔT can be plotted against the H in a T/H diagram. After calculation of all the H values for all the different temperature intervals the hot composite curve can be constructed. Figure 5.1 presents the hot composite curve of the hydrogen production plant (With H_0=10).

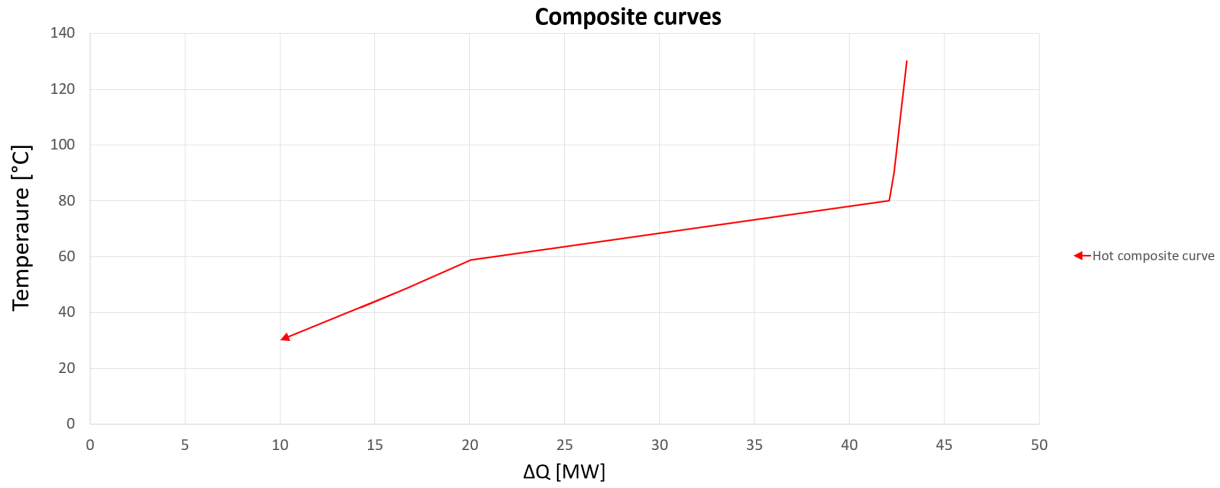

Figure 5.1: Hot composite curve

The stream to be heated, the cold stream, is in this case the stream coming from the heating district that needs to be heated to a certain temperature. This temperature depends on the heating district, but for this analysis a temperature of 85^{o}C is assumed. As the cold composite curve only consists of one stream, the cold composite curve will be a line with constant slope (one single temperature interval). The slope of the line can be changed by altering the mass flows rate and the line can be shifted from left to right in the T/H diagram. The temperature difference at the point where the two curves are closest to one another is called the minimum temperature difference (ΔT_{min}) or the pinch. The temperature related to the centre of the minimum temperature difference is the pinch point. This is where the design is most constrained. Hence, by finding this point and starting the design there, the energy targets can be achieved using heat exchangers to recover heat between hot and cold streams in two separate systems, one for temperatures above pinch temperatures and one for temperatures below pinch temperatures.

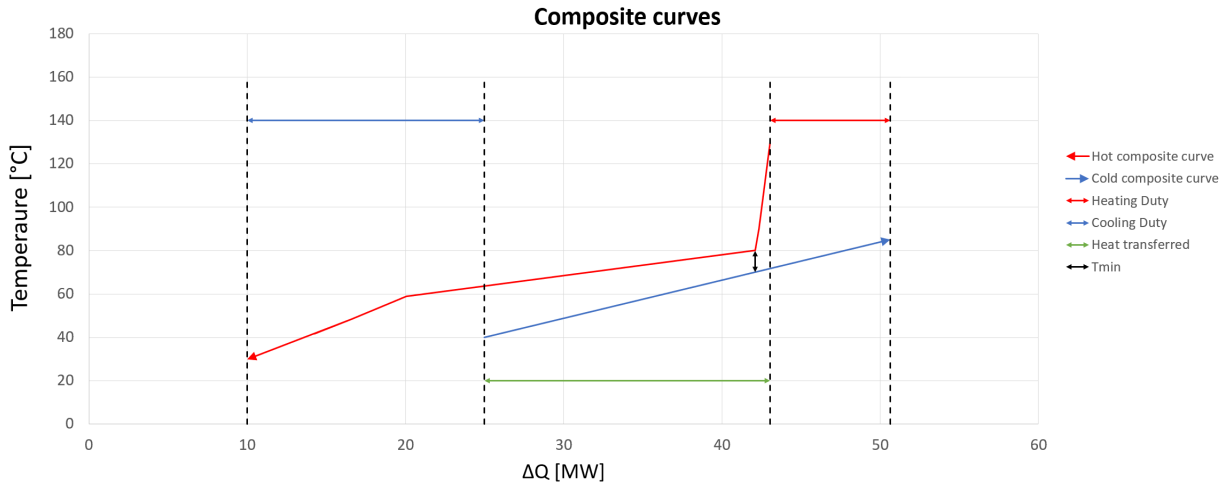

Figure 5.2: Hot and cold composite curves

The overlap between the two composite curves represents the maximum amount of heat recovery possible within the process, the overshoot at the bottom of the hot composite curve (left) represents the external cooling needed and the overshoot at the end of the cold composite curve (right) the external heating that needs to be added. Extra heat can be added with a a heat pump or for example or a gas powered heater. The cooling can be delivered by a cooling tower. Important to note is that the lower quality heat that needs to be cooled (cooling duty) can be used to supply the potential heat pump with energy. Within the heat pump, making use of a compressor, this low quality heat can then be used to

upgrade the to be heated flow to a higher temperature. In this way the overall heat extracted and used from the hydrogen production process is improved by adding compressor power.

5.3. Problem table

The composite curves can be used for obtaining energy targets at a given minimum temperature difference, but a more precise approach for obtaining the precise targets and pinch point is the problem table method first described by Linnhoff and Flower [17]. They describe an algorithm that can be used to find the location of the pinch for a certain heat exchange network and the minimum energy requirements for a specified value of ΔT_{min}. The algorithm starts with setting up the heat content intervals based on supply and target temperatures, but with the hot and cold streams combined. To ensure that the hot and cold streams are at least ΔT_{min} min apart all the temperatures are shifted: $\Delta T_{min}/2$ below hot stream temperatures and $\Delta T_{min}/2$ above cold stream temperatures. Table 5.2 shows the same table as 5.1 but now with the shifted temperatures (S_S S_T) and the cold stream added.

Stream	Hot/Cold	S_S [C]	S_T [C]	Duty [MW]	CP [MW/C]
1	Hot	75	53.88	15.07	0.71
2	Hot	75	25	10.56	0.21
3.1	Hot	125	43.66	0.70	0.094
3.2	Hot	43.66	25	0.50	0.0086
4.1	Hot	125	43.07	0.69	0.027
4.1	Hot	43.07	25	0.28	0.0084
5.1	Hot	84.96	36.77	0.40	0.0084
5.2	Hot	36.77	25	0.14	0.0119
6	Hot	75	25	4.69	0.094
6	Cold	45	90	25.64	0.57

Table 5.2: Shifted stream data

The next step in the algorithm is defining the temperature intervals for heat exchange. In total there are 9 temperature intervals. The first interval is delimited by the hot temperature of stream 3.1 and 4.1 (the cooling in between the compression stages) and the hot temperature from stream 7 (the stream from the heating district). The first interval is from 125^{o}C to 90^{o}C (shifted temperatures). When all the different intervals are found, the problem table (table 5.3) can be constructed. In the problem table the first column gives the temperature intervals, the second column the interval number, the third column the temperature difference for the specific interval, column five gives the sum of the CP values of the active streams in the specific interval and column six gives the energy balance of the interval.

$$\Delta H_i = (S_i - S_{i+1})\big(\sum CP_H - \sum CP_C\big)_i \tag{5.4}$$

The last column in the problem table give a qualitative message: a negative value signifies heat surplus, while a positive value means a deficit. Excess heat can be removed by cold utility and the deficit in certain intervals can be supplied by hot utility. Instead of this poor energy use option, the idea is to combine heat content from different intervals.

Temp	Interval i	Si-Si+1	CPh-CPc	Hi	Surpl/Def
125					
	1	35	0.02	0.60	Surplus
90					
	2	3	-0.55	-1.85	Deficit
87					
	3	12	-0.54	-6.34	Deficit
75					
	4	21	0.53	11.12	Surplus
54					
	5	9	-0.27	-2.37	Deficit
45					
	6	1	0.30	0.45	Surplus
44					
	7	1	0.32	0.19	Surplus
43					
	8	6	0.33	1.91	Surplus
37					
	9	12	0.33	3.95	Surplus
25					

Table 5.3: Problem table

The coupling of the intervals is done in a cascading manner as shown in table 5.4. In a first trial (table 5.4, left), we assume that no heat is transferred from the hot utility. The first interval has an excess of 0.6 MW that can be transferred to the second one, resulting in a net energy flow of 0.6 MW. The second interval has a deficit of 1.85 MW, so that the net heat flow after this interval becomes -1.26 MW ($0.6 - 1.85$). The third interval has a deficit of 6.34 MW. Clearly, a negative heat flow (-1.26 MW) cannot be cascaded further. Therefore, this solution is not feasible.

Temp	H	Hflow
125		0
	0.60	
90		0.60
	-1.85	
87		-1.26
	-6.34	
75		-7.60
	11.12	
54		3.52
	-2.37	
45		1.15
	0.45	
44		1.60
	0.19	
43		1.79
	1.91	
37		3.70
	3.95	
25		7.66

Temp	H	Hflow
125		7.60
	0.60	
90		8.19
	-1.85	
87		6.34
	-6.34	
75		0.00
	11.12	
54		11.12
	-2.37	
45		8.75
	0.45	
44		9.20
	0.19	
43		9.39
	1.91	
37		11.30
	3.95	
25		15.26

Table 5.4: Cascade table

In a second trial, we may consider a hot utility load of 7.60 MW that could compensate the deficit noted before. The result of cascading heat flow can be seen in table 5.4 (right). After the first interval, the net heat flow is 7.60 + 0.60 = 8.19 MW. The second interval delivers 8.19 - 1.85 = 6.34 MW. The cascade

of heat flow goes on until the lowest interval is reached. As it can be seen, now all the net flows but one is positive. The location where the heat flow is zero is the Pinch Point. The shifted temperature is of 75 or 70 - 80^{o}C expressed in real-stream temperatures.
From the cascade diagram the hot utility (7.6 MW), cold utility (15.26 MW) and pinch point (75^{o}C) can be read. Comparing the found results with the composite curves shown in figure 5.2, it is apparent that the overshoot o the left (cold utility), the overshoot on the right (hot utility) and the pinch point correspond with the found values.

5.4. Design of the heat exchange network

For designing a heat exchanger network, the most helpful representation is the “grid diagram” introduced by Linnhoff and Flower (1978). The streams are drawn as horizontal lines, with high temperatures on the left and hot streams at the top; heat exchange matches are represented by two circles joined by a vertical line. There are three important rules when designing the network: 1. No heat exchange across the pinch, 2. Not hot utility below the pinch, 3. Not cold utility above the pinch. The Pinch splits the diagram into two regions: above (at the left) and below (at the right) the Pinch. The design starts at the Pinch, where the heat transfer is the most constrained. The match procedure has to respect some feasibility rules. Above the pinch $CP_{hot} \leq CP_{cold}$ and below the pinch $CP_{hot} \geq CP_{cold}$. Figure 5.3 shows the design of heat exchange network represented in a grid diagram.

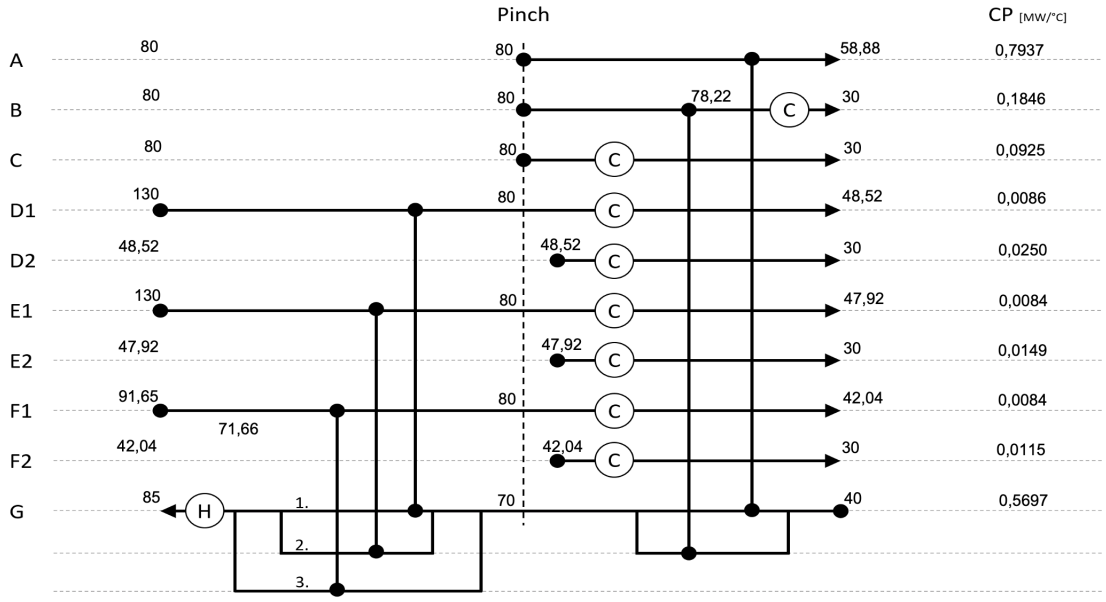

Figure 5.3: Heat exchange network represented as grid diagram

From the found grid diagram a design for the process flow diagram of the thermal extraction part of the hydrogen production plant can formed. Figure 5.4 shows the found grid diagram translated to a PFD. As can be seen in the grid diagram, the heat exchangers above the pinch only upgrade the quality of the heat from 70 to 71.04^{o}C. This would be a large investment for only a small upgrade. For this reason the choice was made to exclude these heat exchangers which will increase the duty of the hot utility.

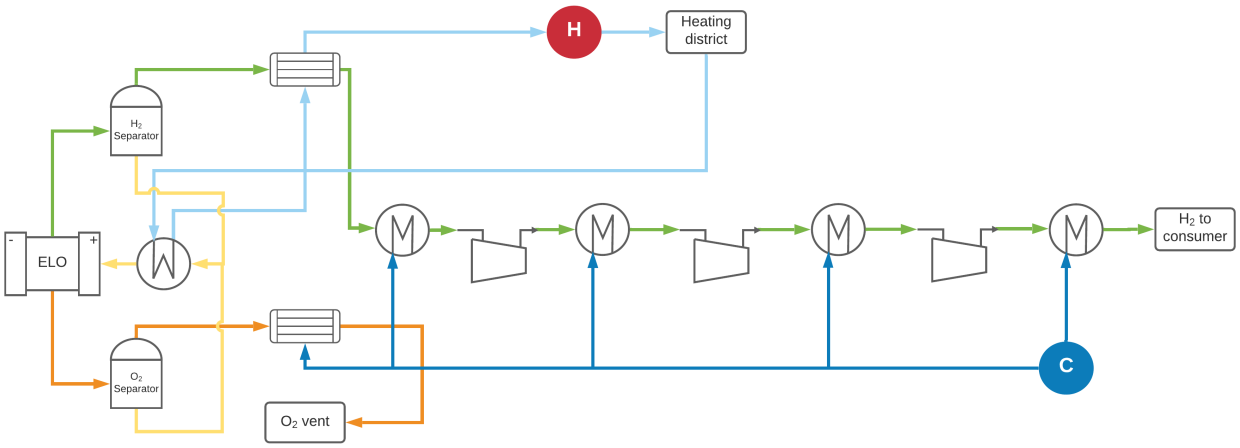

Figure 5.4: Process flow diagram found after pinch analysis (scenario 1.)

In figure 5.4 the yellow line represents the flow of lye, the green line the flow of hydrogen/steam, the orange line the flow of oxygen/steam, the light blue line the flow of district heating water and the dark blue line the flow from the cold utility. The hot utility (the red dot) needs to upgrade the quality of the heat from 70 to 85^{o}C. The cold utility (blue dot) needs to make sure that sufficient cooling is provided.

It would be wasteful to discard the thermal energy that is cooled away by the cold utility. A solution for this is to use this thermal energy to feed the source side of a heat pump. This way by adding some compressor power the thermal energy can be used to upgrade the district heating water to the desired temperature of 85^{o}C. Figure 5.5 shows the final design of the thermal extraction and utilisation system for scenario 1 with the inclusion of a heat pump as well as a thermal storage system.

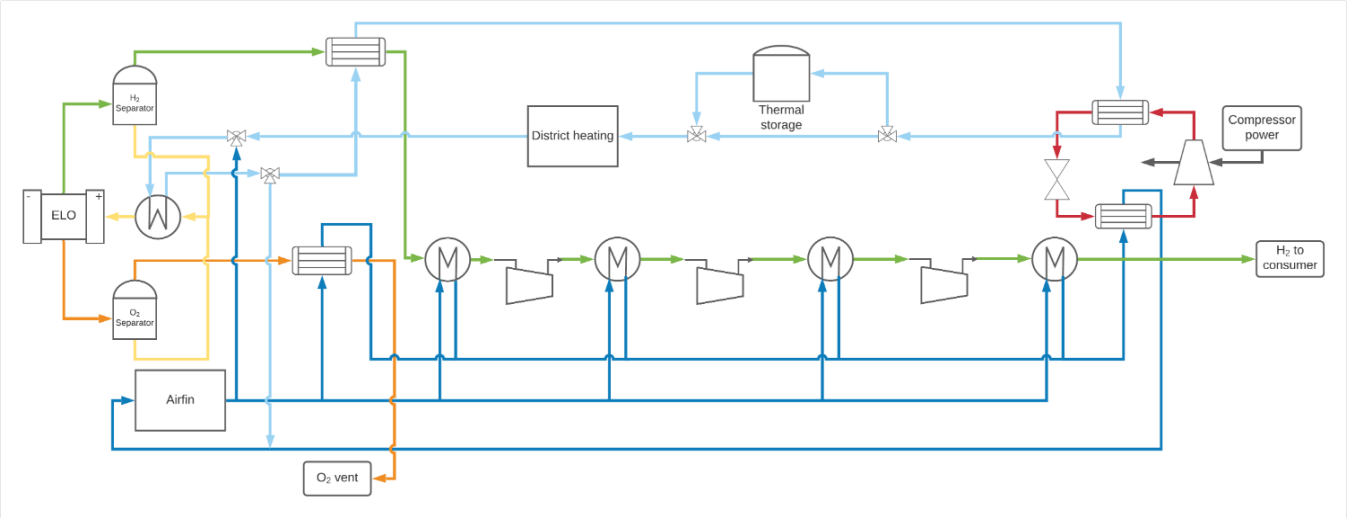

Figure 5.5: Process flow diagram found after pinch analysis (scenario 1.) with added heat pump and storage

When demand from the heating district is low, the 85^{o}C district heating waster can be stored for when thermal demand is high. For a cold utility an air fin cooler system is selected. The advantage of an air fin cooler system is that it is a closed circuit system. Because of this, as a cooling liquid the district heating water may be used and problems of mixing different cooling liquids do not arise.

6

Results & Discussion

Using the described thermal model (section 3), the different scenarios are analysed. This section will present the results and discuss their meaning and implication. For every scenario the criteria described in section 1.3.1 are calculated and reviewed:

- Electrolyser efficiency
- Fraction of generated thermal energy recovered
- Overall efficiency
- Fraction of normal household gas use needed
- Fraction of the thermal energy recovered used
- Investment cost
- CO_2 avoided
- Euro invested per yearly CO_2 avoided

Every scenario is analysed for start of life, middle of life and end of life. For every scenario the results of the pinch analysis are also discussed as well as the sizing of the equipment. Resulting from the equipment sizing the CAPEX of the different scenarios is discussed.

Table 6.1 shows the characteristics of the four different evaluated scenarios. 'Power in' indicates whether the hydrogen plant follows the pattern of the wind farm or whether the plant operates under a baseload of 70MW and only the remaining 30MW follows the pattern of the wind farm. 'HP' indicates whether a heat pump is used in the design, the 'demand temp' indicates the temperature needed in the heating district and the 'PFD' gives what PFD design is used (see chapter 5).

$$\dot{Q}_{recov} = \dot{Q}_{elec,cool} + \dot{Q}_{H_2,cond} + \dot{Q}_{HP,evap} \tag{6.1}$$

$$\dot{Q}_{recov} = \dot{Q}_{elec,cool} + \dot{Q}_{H_2,cond} + +\dot{Q}_{O_2,cond} \tag{6.2}$$

$$Recov - fraction = \frac{\dot{Q}_{recov}}{\dot{Q}_{gen}} \tag{6.3}$$

	Scenario 1	Scenario 2	Scenario 3	Scenario 4
Power in	Fluctuating	70% Baseload	Fluctuating	70%Baseload
Elec temp	80C	80C	80C	80C
HP	Yes	Yes	No	No
Demand temp	85C	85C	70C	70C
PFD	1	1	2	2

Table 6.1: Scenario characteristics

6.1. Process flow diagram

The results of the pinch analysis are presented in this section. Based on the demand temperature two different PFD's where found as described in chapter 5.

6.1.1. PFD: For scenario 1 and 2

The result of the pinch analysis for when the demand temperature is 85^{o}C (scenario 1 and 2) is obtained in chapter 5. The result is shown in figure 6.1

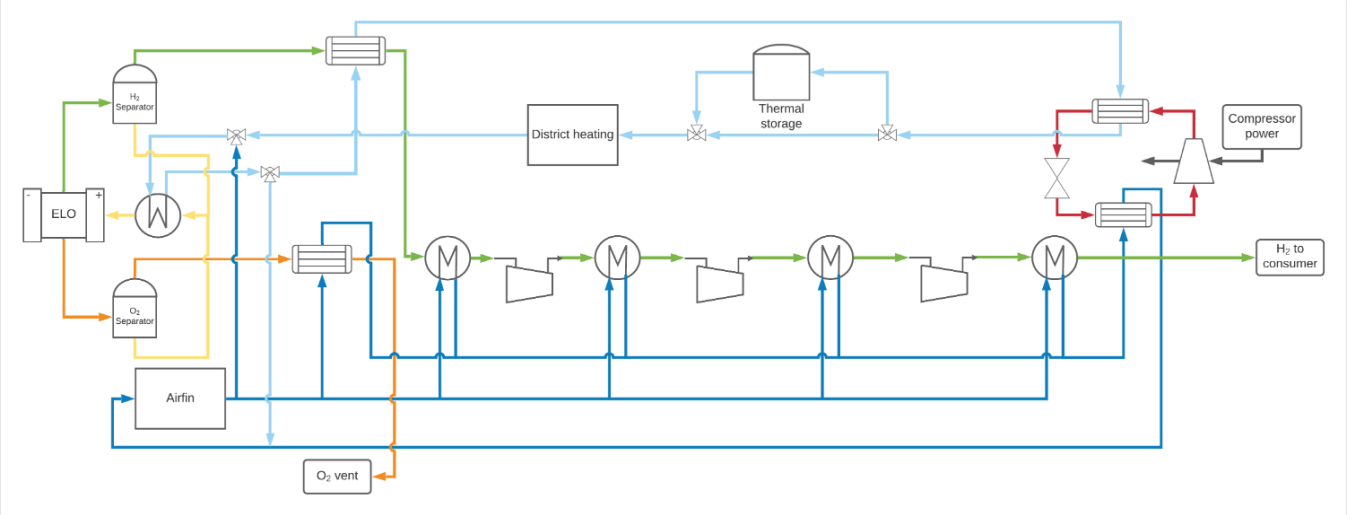

Figure 6.1: Process flow diagram found after pinch analysis (scenario 1.) with added heat pump and storage

In this design, the district heating water (light blue) is heated up to 70 degrees Celsius by the electrolyte flow (yellow) from the separators and thereafter by the hydrogen condenser. The heat pump heats the district heating water to 85 degrees Celsius on the condenser side (sink). The evaporator side of the heat pump (source) is also fed by heated district heating water (dark blue). This district heating water is heated by the oxygen condenser and heat exchangers in between the compressor. After delivering thermal energy to the heat pump, this dark blue district heating water is cooled by a airfin cooler. This circuit (dark blue) is also able to deliver cooled district heating water to the electrolyte cooler via a three way valve. This ensures sufficient cooling for the electrolyser for the district heating water from the district is not cool enough.

6.1.2. PFD: For scenario 3 and 4

By changing the temperature from 85 to 70^{o}C in the pinch analysis the cold composite curve changes while the hot composite curve stays the same. Figure 6.2 shows the composite curves.

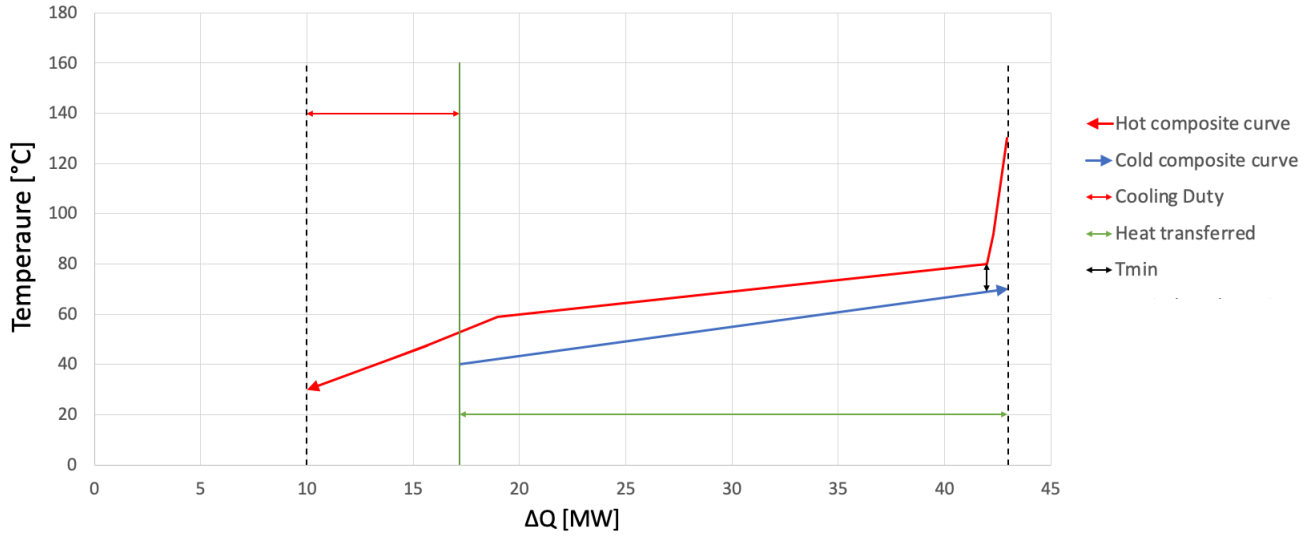

Figure 6.2: Composite curves for scenario 2.

The flow from the heating district is set to 200 kg/h. From the curves it can be seen that only the last few degrees are delivered by the flows that operate at temperatures above 80^{o}C and from the analysis of scenario 1. it became apparent that this would require a large investment while gaining just a little. By downsizing the flow just a little and moving the cold composite curve to the left it can be made sure that only the flows below 80^{o}C are needed to upgrade the flow form the heating district to the required temperate of 70^{o}C which also means that no heat pump will be required.

Repeating the steps discussed in the chapter on pinch analysis the process flow diagram shown in figure 6.3 was designed.

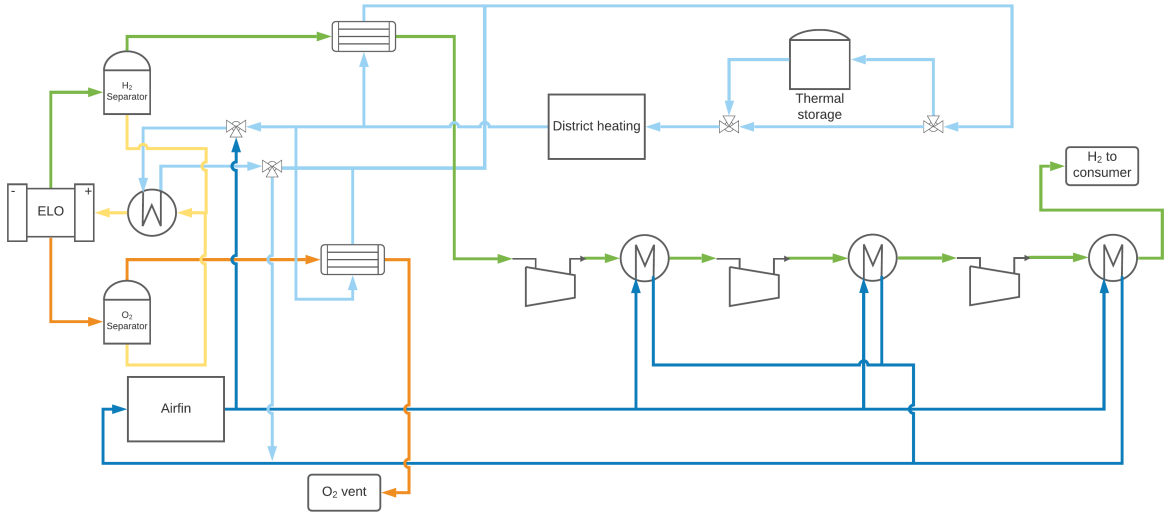

Figure 6.3: Process flow diagram for scenario 2

In this design the thermal energy from the hydrogen condenser, oxygen condenser and lye cooler are used to upgrade the district heating water from 40 to 70^{o}C and the extra heat exchangers that was previously necessary before the first compressor can also be omitted. This will mean that the first compressor will be a little less efficient since the flow from the district heating water is only 40^{o}C and thus can the hydrogen flow not be cooled to 30^{o}C.

6.2. Electrolyser efficiency

Figure 6.4 shows the electrolyser efficiency (η_{elec}, equation 3.62) and the input power ($P_{windfarm}$) and the heat generated in the electrolyser ($\dot{Q}_{gen}$, equation 3.25). It is apparent that when the plant becomes older the efficiency (orange) decreases since more thermal energy (blue) is generated.

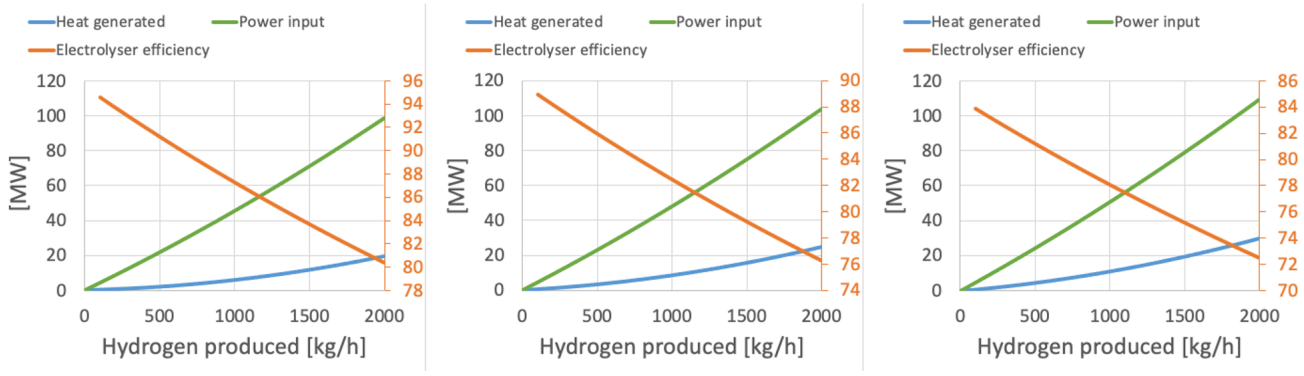

Figure 6.4: Electrolyser efficiency (from left to right: Start life, middle life, end life)

6.3. Fraction of generated thermal energy recovered

Here the amount of thermal energy is presented that is recovered from the hydrogen production plant. Since the result is PFD dependent the graphs are the same for scenario 1 and 2 and for 3 and 4.

6.3.1. For scenario 1 and 2

Figure 6.5 shows the amount of thermal energy that is extracted ($\dot{Q}_{recov}$) and directly added to the district heating water (before heat pump) as a function of the amount of hydrogen produced for the different lifetimes of the hydrogen production plant. This thermal energy is used to upgrade the flow of district heating water form 40 tot 70^{o}C. The remaining 15^{o}C will need to be delivered by the heat pump (see next paragraph). It also shows the total amount of thermal energy that is generated in the electrolyser. In scenario 1 and 2, $\dot{Q}_{recov}$ is the thermal energy extracted using the lye cooler and the hydrogen condenser. The total amount of thermal energy recovered is the thermal energy directly recovered plus the amount that is recovered by the evaporator side of the condenser. The $Recov - fraction$ is calculated via:

$$Recov - fraction = \frac{\dot{Q}_{lye,cool} + \dot{Q}_{H_2,cond} + \dot{Q}_{evap,HP}}{\dot{Q}_{gen}} \tag{6.4}$$

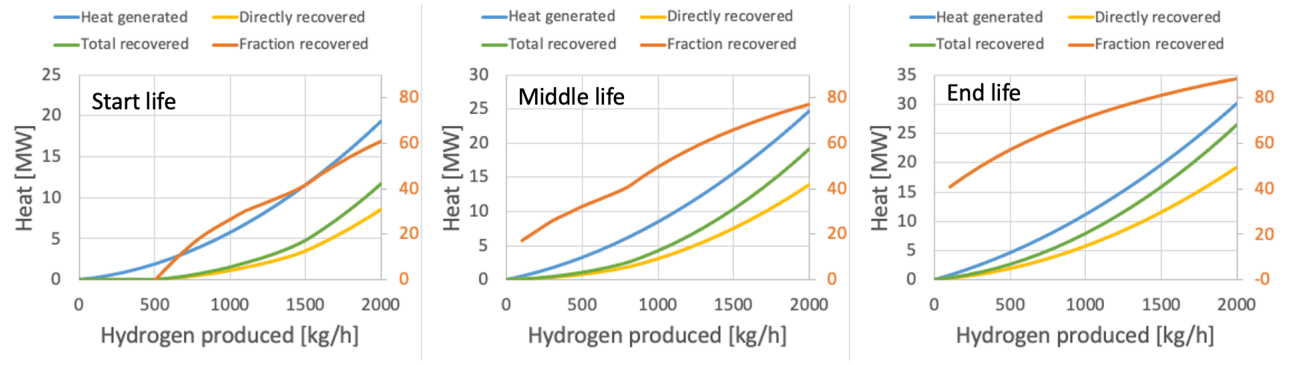

Figure 6.5: Fraction of total heat generated recovered (from left to right: Start life, middle life, end life)

It can be seen that the amount of thermal energy generated grows exponentially with the amount of hydrogen produced. Looking at equation 3.25 this is what you would expect, since both the current and the cell potential are growing. The total thermal energy directly extracted also grows exponentially with the amount of hydrogen produced.

Highest fraction of the generated heat recovered is at end of life and full capacity (88%). Looking at figure 6.4, it can be seen that the electroyser efficiency is also highest at full capacity, but not at end of life. At start of life and full capacity the highest efficiency can be realised.

6.3.2. For scenario 3 and 4

All the thermal energy that is extracted and put to use is directly added to the district heating flow to reach the desired temperature of 70^{o}C. Figure 6.6 shows the amount of thermal energy that is extracted for all the lifetimes. It can be seen that almost all the energy generated is extracted when using this design.

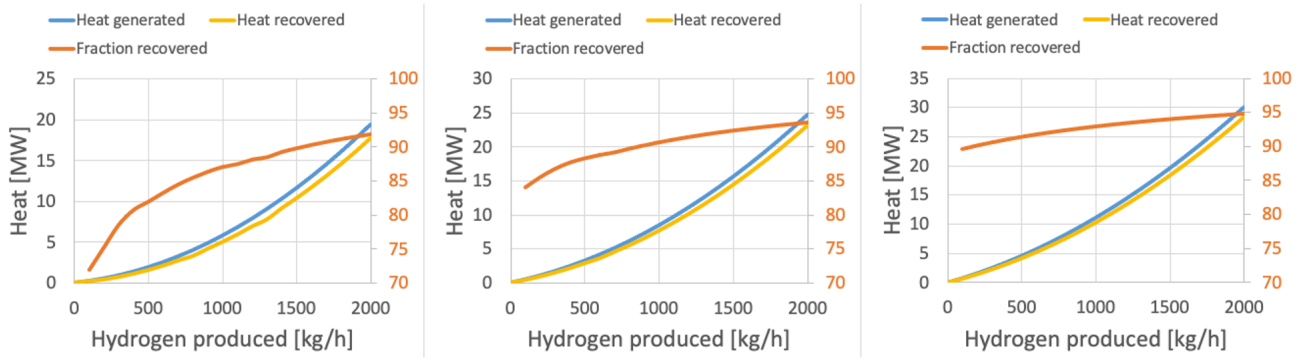

Figure 6.6: Thermal energy extracted in scenarios 3 and 4

Highest fraction of the generated heat recovered is at end of life and full capacity (95%). Looking at figure 6.4, it can be seen that the electroyser efficiency is also highest at full capacity, but not at end of life. At start of life and full capacity the highest efficiency can be realised.

Comparing figure 6.5 and 6.6 (85 vs 70 demand temperature) shows that more of the generated thermal energy can be recovered when the demand temperature is lower (88% vs 95% when looking at maximum recovery). Also, no HP is needed for realising the 95% recovery at end of life.

6.4. Overall efficiency

The overall efficiency is calculated as described by equation 3.64 and the results are presented in figure 6.7. It can be seen that the overall efficiency is fairly constant during all capacities (hydrogen production). For start and middle of life the overall efficiency decreases at first, this is because the amount of generated heat increases faster than the amount of heat recovered up to a turning point.

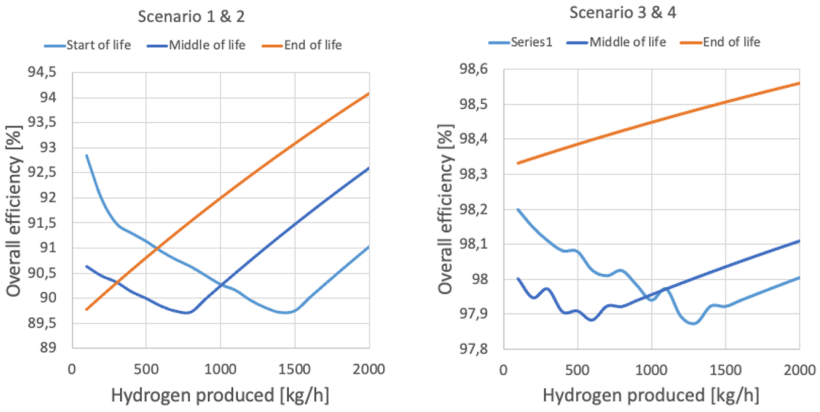

Figure 6.7: Overall efficiency

Comparing the found overall efficiency with the electrolyser efficiency (figure 6.4) is can be seen that adding the thermal system increases the efficiency significantly. For scenario 1 and 2, the overall efficiency lies around 90% for all operational capacities and for scenario 3 and 4 even higher, around 98%. The wobbly lien is because the differences in efficiency are very small and are due to the data used for the water saturation pressure.

6.5. Investment cost

In this section the cost for adding the thermal extraction and utilisation system is discussed. For this study the heat exchangers, heat pump, thermal piping from plant to heating district and thermal storage are included. It should be noted that some heat exchangers would be installed even without having maximum thermal extraction as a goal.

Heat exchangers

For scenario 1 and 2 a total of seven heat exchangers are needed (figure 6.1). Table 6.2 shows the relevant parameters for when the plant operates at full capacity and when the electrolysers are at the end of their lifetime (8 years). By doing this, the heat exchangers are calculated for the maximum load that they may need to carry. The surface needed for heat exchange is calculated for every heat exchanger based on equation **??** and the cost for equipment (C_e) and the total cost (equipment plus installation, C) is calculated using equations 3.57 and 3.58.

HEX	Tm	U	Q	A	C_e[$]	C [$]
Lye cooler	14.36	5750	15.70	190	27683	96892
H2 Cooler 1	22.21	4000	3.92	44	7928	27750
H2 Cooler 2	9.00	4000	4.32	120	18355	64241
Compr Cooler 1	21.27	4000	1.09	12	3379	11828
Compr Cooler 2	21.27	4000	0.91	10	3059	10708
O2 Cooler	8.96	4000	4.77	132	20092	70323

Table 6.2: Cost for heat exchangers in scenario 1

In total this amounts to a price of 286469 dollars. It should be stated that is estimates the price as being on a U.S. Gulf Coast basis, January 2007. Using the CEPSI cost index (525.4 for 2007 and 655.9 for 2021) and equation 3.59 to adjust for inflation gives 357624 dollars which is equal to 303753 euros.

For scenario 3 and 4 (6.3), only the heat exchangers that cools the hydrogen before entering the first compressor changes. H2 cooler 1 and 2 become one heat exchanger that uses the district heating water as cooling liquid. Since the rest of the heat exchangers remain, the cost will also stay the same.

HEX	Tm	U	Q	A	C_e[$]	C [$]
H2 Cooler	4.97	4000	8.04	404.55	55289	193511

Calculating the new cost for all the necessary heat exchangers gives a total price of 357806 dollars which is equal to 379392 euro in 2021.

Air fin cooling
At maximum capacity (end of life, 2000 kg/h), the air fin cooling system needs to cool the flow that comes form the evaporator to 30^{o}C. It also needs to provide extra cooling in case the heating district does not cool the district heating water sufficiently so that the electrolyser does not overheat. At maximum capacity the flow from the evaporator is around 80 kg/s. At maximum capacity cool water flow to the lye cooler is around 120 kg/s. This gives a total of 200 kg/s. Using the equation 3.57 and the values in table AAA an estimation is made for the total cost of the air fin cooling system. The total amount C_e is equal to 303063 dollars. Using the CEPSI cost index to correct for inflation gives 378338 dollars (321347 euros).

Heat pump
At maximum capacity the heat pump needs to deliver around 10 MW. From figure 3.12 it can be seen that such a heat pump requires an investment of an estimated amount of 3 million euros (3.54 million dollar).

Thermal storage
From figure 3.11 the cost for thermal pit storage can be found in euros per cubic meter water equivalent. For a thermal storage of 5000 m^3 the storage cost per cubic meter is equal to 100 euros which gives a total cost of 500000 euros. A smaller storage (500 m^3) will cost around 300 euros per cubic meter which equals to 150000 euros.

Piping
Using the total length from the plant to the location of Velsen-Noord (3 km), the maximum transferred heat ($\dot{Q}$ and equation 3.60 and 3.61 the minimum and maximum cost for the installation and cost for the piping of the heating district can be estimated. At full capacity and in when the plant is 4 years old $\dot{Q}$ is equal to 55 MW (155 kg/s at 85^{o}C). This gives an CAPEX$_min$ of 1957 euros per meter and a CAPEX$_max$ of 3014 euros per meter which on average is equal to 2485 euros per meter. For a piping length of 3 km this comes down to a investment of 7.5 million euros (average used).

Total cost
Adding all the cost for the different components for the thermal system a total cost of 11.8 million euros is found for the design given by figure 6.1 (scenario 1 and 2). This is the sum of the cost for heat exchangers, the heat pump, the thermal storage and the piping.

For scenario 3 and 4 the total sum gives an estimate of 8.9 million euros. The difference is mainly a result of the omission of a heat pump in the design.

6.6. MW recovered per million invested

Since the total investment cost and the amount of extracted thermal energy is known, the recovered thermal energy per invested euro can be plotted (figure 6.8).

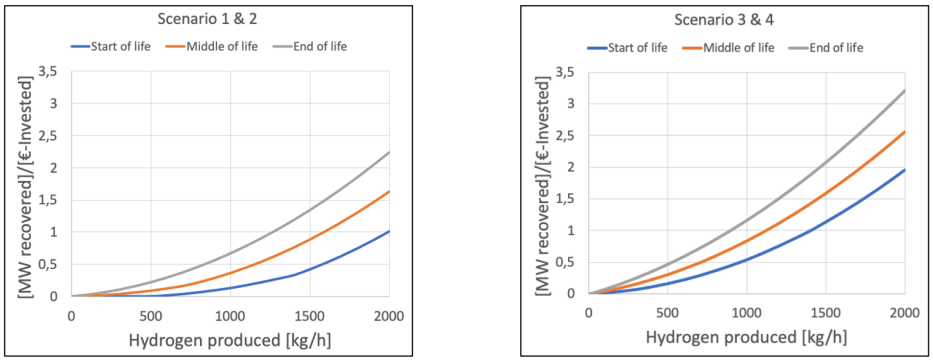

Figure 6.8: Thermal energy recovered per euro invested

Based on the plots can be seen that more energy is recovered per euro invested when the plant operates at a higher capacity and that this also increases with the age of the plant. What also is observed is that the amount of energy extracted per invested euro is higher for scenario 3 and 4 than for 1 and 2 for every plant capacity.

6.7. Fraction of normal gas use needed

This section shows the reduction in gas use based in the amount of houses in the thermal heating district and for different storage sizes. Subsequently, the amount of CO_2 reduction is calculated and plotted.

6.7.1. Scenario 1

Figure 6.9 shows the influence of the thermal storage as a function of the number of houses (left). The influence of multiple storage sizes is modelled. The influence is measured by looking at the percentage of the yearly gas use that is still needed to provide sufficient thermal energy. It can be seen that the influence o thermal storage reduces as the storage becomes larger and also when the amount of houses in the district becomes larger.

When infinite storage is used, up to around 2500 houses could be totally gas free. Figure 6.9 also shows the reduction in CO_2 use for every household in the heating district. When no gas use is needed, this results in a reduction of around 36% in total CO_2 emissions.

For Velsen-Noord (indicated by the black vertical line), adding 3000 m^3 of storage, can almost ensure the independence on gas. Also adding just 250 m^3 greatly reduces the gas use for Velsen-Noord (15%).

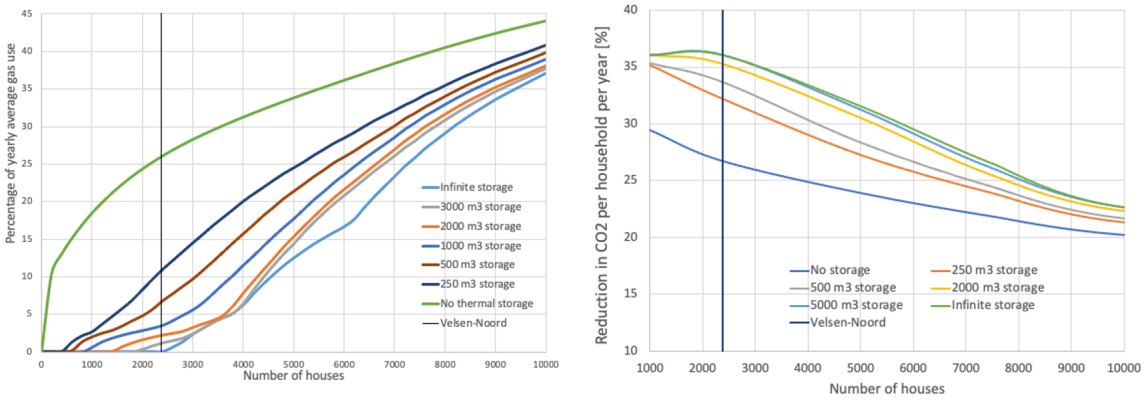

Figure 6.9: Left: Yearly gas use as a function of number of houses for different storage sizes, Right: Reduction in CO_2 emissions

6.7.2. Scenario 2

Since during the year the plant always operates at a minimum of 70 MW, the overall available thermal energy during the year is much higher. Figure 6.11 shows the percentage of the yearly gas needed as a function of the number of houses.

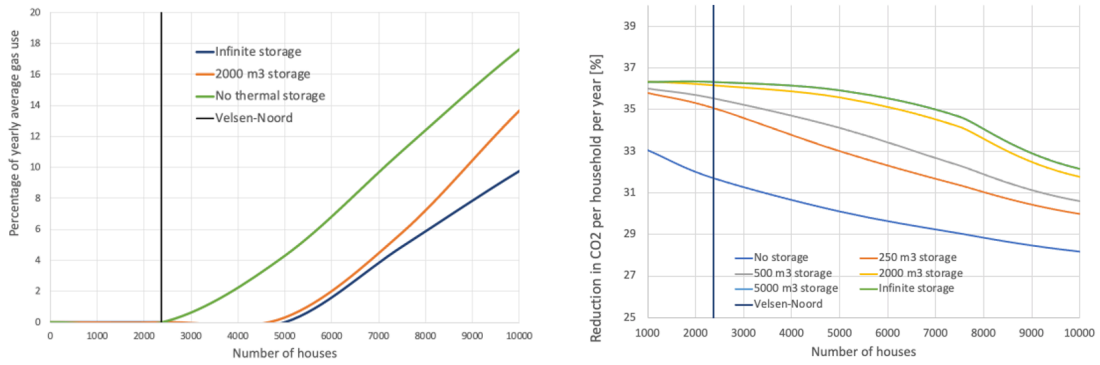

Figure 6.10: Left: Yearly gas use as a function of number of houses for different storage sizes, Right: Reduction in CO_2 emissions

In this scenario the use of thermal storage is much less significant than for scenario 1. Is can be seen that adding thermal storage for the situation of Velsen-Noord would not benefit gas reduction since no gas is needed even without storage.

It can be seen that when no gas is needed, around 36% of the average CO_2 emissions are avoided.

6.7.3. Scenario 3

Figure 6.10 shows the percentage of gas needed of the average yearly gas use as a function of the number of houses. It can be seen that even with no thermal storage for 10000 houses only 22,5% of the yearly gas use that normally (without thermal energy from the proposed system) would be used for 10000 houses is necessary. Just like with scenario 1, adding only 250 m^3 of storage, reduces the amount of gas needed even more (±20% for Velsen-Noord). With a storage size of 3000 m^3, Velsen-Noord would be completely independent of gas and would reduce the CO_2 emissions with ±36%.

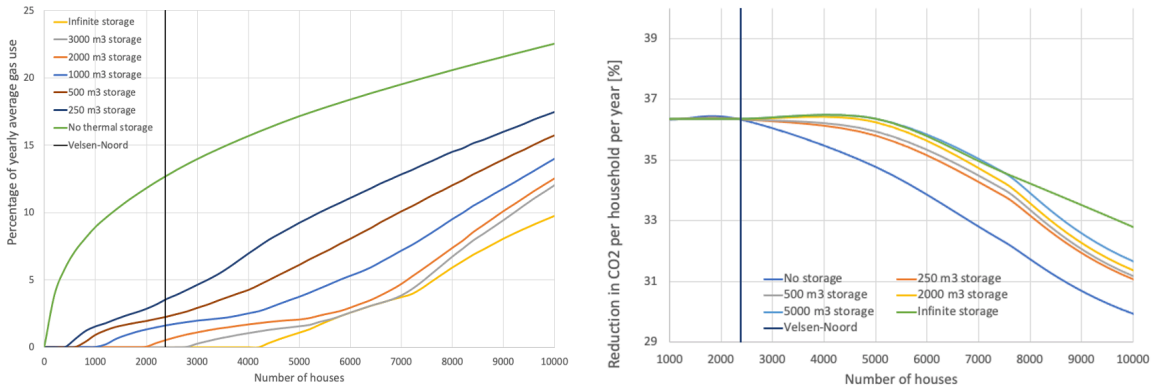

Figure 6.11: Left: Yearly gas use as a function of number of houses for different storage sizes, Right: Reduction in CO_2 emissions

6.7.4. Scenario 4

Since during the year the plant always operates at a minimum of 70 MW, the overall available thermal energy during the year is much higher. Figure 6.11 shows the percentage of the yearly gas needed as a function of the number of houses.

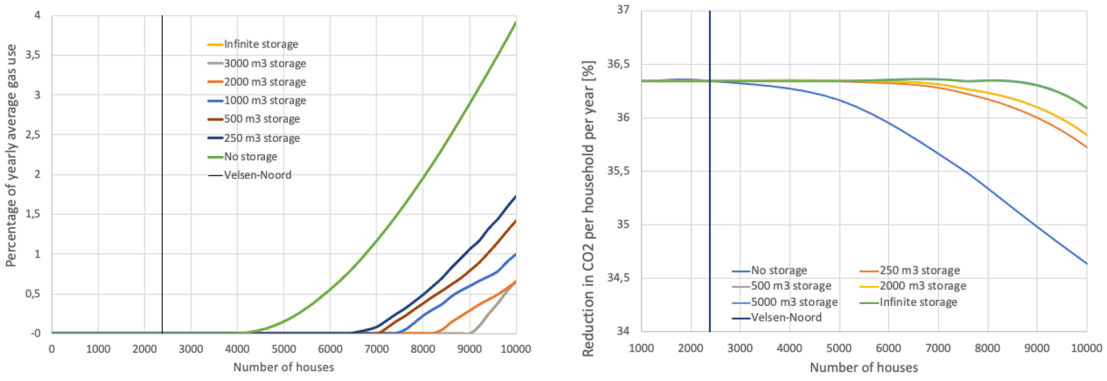

Figure 6.12: Left: Yearly gas use as a function of number of houses for different storage sizes, Right: Reduction in CO_2 emissions

In this scenario the use of thermal storage is much less significant than for scenario 3. Is can be seen that adding thermal storage for the situation of Velsen-Noord would not benefit gas reduction since no gas is needed even without storage.

6.8. Overview results

This section gives an overview of the discussed criteria for all the different scenarios. Table 6.3, 6.5 and 6.4 give the outcome of the criteria that tell something about the efficiency and the amount of thermal energy that can be extracted form the hydrogen production plant in relation to the production rate of hydrogen. The tables are divided in start, middle and end of life and shows the results for the four different scenarios. For every scenario the results are shown relative to the capacity which is given in percentages. Here 100% refers to the case when the plant operate at full capacity (100 MW).

From the results can be seen that the efficiency of the electrolyser (η_{elec}) declines when the capacity increases. This is because more energy is lost due to heat generation. η_{elec} is not dependent on the different scenarios since the electrolyser conditions remain constant. However, the efficiency does decline when the age of the hydrogen plant increases. The difference in electrolyser efficiency between start and end of life is 7.9% for full capacity.

$D-R-F$ ($Direct-recov-fraction$) shows the percentage of thermal energy that is directly recovered (without heat pump). $R-F$ ($Recov-fraction$) is the total percentage of the generated thermal energy that is extracted. For all scenarios and ages of the hydrogen plant it can be seen that when the capacity increases the amount of extracted thermal energy increases as well. For scenario 1 and 2, start of life (table 6.3) it shows that no generated thermal energy is extracted at a capacity of 25%. This is because all the thermal energy that is generated is needed to maintain a temperature of 80^{o}C in the electrolyser. For scenario 3 and 4 the $D-R-F$ and $R-F$ are equal since no heat pump is included in that scenario.

P_{ext} is the external power needed to realise the $R-F$. In the discussed scenarios this is the power needed for compression in the heat pump. The results show that by adding a relatively small amount of external power (and thus making use of a heat pump) a much larger percentages of thermal energy can be extracted (difference between $D-R-F$ and $R-F$).

η_{tot} is the total efficiency of the system which is the energy used for the formation of hydrogen and oxygen plus the total mount of thermal energy extracted over the inputted power. Table 6.3, 6.5 and 6.4 show that η_{tot} lower for scenario 1 and 2 and that η_{tot} is higher for scenario 3 and 4.

C_{invest} gives an estimation of the investment cost needed to realise the thermal extraction system. Scenario 3 and 4 are 2.9 million euros cheaper than 1 and 2 since the use of a heat pump is excluded.

Start of life	Scenario 1 & 2				Scenario 3 & 4			
Capacity [%]	25	50	75	100	25	50	75	100
η_{elec} [%]	91.2	87.3	83.7	80.4	91.2	87.3	83.7	80.4
$D-R-F$ [%]	0	19.4	38.5	49.7	78.0	84.2	87.5	90.0
$R-F$ [%]	0	26.6	44.3	62.9	78.0	84.2	87.5	90.0
P_{ext} [MW]	-	0.18	0.60	1.42	-	-	-	-
η_{tot} [%]	91.2	90.3	90.2	91.4	98.1	98.0	97.0	98.0
C_{invest} [mil]	11.8				8.9			

Table 6.3: Criteria for start of life

Middle of life	Scenario 1 & 2				Scenario 3 & 4			
Capacity [%]	25	50	75	100	25	50	75	100
η_{elec} [%]	85.9	82.4	79.2	76.2	85.9	82.4	79.2	76.2
$D-R-F$ [%]	24.0	38.2	49.8	57.7	88.3	90.7	92.4	93.6
$R-F$ [%]	32.8	52.2	68.1	78.9	88.3	90.7	92.4	93.6
P_{ext} [MW]	0.12	0.51	1.24	2.27	-	-	-	-
η_{tot} [%]	90.0	90.6	91.9	93.0	98.4	98.4	99.4	99.2
C_{invest} [mil]	11.8				8.9			

Table 6.4: Criteria for middle of life

End of life	Scenario 1 & 2				Scenario 3 & 4			
Capacity [%]	25	50	75	100	25	50	75	100
η_{elec}[%]	81.2	78.1	75.2	72.5	81.2	78.1	75.2	72.5
$D-R-F$ [%]	41.8	51.0	59.1	64.4	89.5	91.3	94.0	94.8
$R-F$ [%]	58.9	72.6	82.2	89.2	89.5	91.3	94.0	94.8
$P_{ext}[MW]$ [%]	0.32	0.94	1.88	3.12	-	-	-	-
η_{tot} [%]	91.1	92.3	93.4	94.3	98.0	98.1	98.2	98.2
C_{invest} [mil]	11.8				8.9			

Table 6.5: Criteria for end of life

Table 6.6, 6.7 and 6.8 give the outcome of the criteria that reflect the influence of the thermal storage as a function of the number of houses that are supplied with thermal energy and the storage size. V-N stands for the case study of Velsen-Noord (2372 houses).

$Gas-fraction$ gives the percentage of the gas that is normally consumed by the amount of houses reviewed per year still needed after addition of the thermal extraction system and thermal storage. So 100% - '$Gas-fraction$' gives the reduction in yearly gas use. For scenario 1 can be seen that for the Velsen-Noord case study the addition of 2000 m^3 reduces the $Gas-fraction$ to zero. The results also show that the when the number of houses is increases, the influence of thermal storage reduces.

$Used-fraction$ gives the percentage of the extracted thermal energy that is actually used. Adding thermal storage closes the gab between supply and demand and increases $Used-fraction$. Also here, when the number of houses increases, the influence of adding thermal storage on $Used-fraction$ decreases.

The amount of CO_2 that is avoided ($CO_2-avoid$, in tonnes) is the reduction in CO_2 emission due the fact that less natural gas is needed to provide households with thermal energy throughout the year as a result of the added thermal system. Both increasing the number of houses as the size of the thermal storage increase $CO_2-avoid$. But as well for this criteria, it only increases up to a certain point. it can be seen that there is almost no increase in $CO_2-avoid$ between storage of 5000 m^3 and an infinite storage size and when the amount of houses becomes large, the storage size does not have a positive influence anymore.

From $CO_2 - avoid$ and C_{invest} the amount of CO_2 avoided per invested euro is calculated (€/$CO_2 - avoid$). For 50000 houses this value is very small (233 €/t) compared to when only 1000 houses are supplied with thermal energy (5350 €/t for no thermal storage). But for 1000 houses much more CO_2 is avoided per household: 2,205 tonnes compared to 1.015 tonnes per household for 1000 and 50000 houses respectively.

# Houses		Scenario 1					
	Storage size [m^3]	0	250	500	2000	5000	∞
1000	$Gas - fraction$ [%]	18.5	2.6	2.0	0	0	0
	$Used - fraction$ [%]	15.7	20.6	20.9	21.5	21.5	21.5
	$CO_2 - avoid$ [t]	2205	2636	2652	2706	2706	2706
	€/$CO_2 - avoid$ [€/t]	5350	4477	4450	4361	4361	4361
V-N	$Gas - fraction$ [%]	26.0	10.8	6.6	2.2	0	0
	$Used - fraction$ [%]	31.7	42.9	46.0	49.3	50.9	50.9
	$CO_2 - avoid$ [t]	4750	5725	5995	6277	6419	6418
	€/$CO_2 - avoid$ [€/t]	2484	2061	1968	1880	1838	1838
5000	$Gas - fraction$ [%]	33.8	24.5	21.4	15.4	13.4	12.5
	$Used - fraction$ [%]	54.6	69.2	74.0	83.4	86.5	97.9
	$CO_2 - avoid$ [t]	8957	10215	10634	11446	11717	11838
	€/$CO_2 - avoid$ [€/t]	1317	1155	1110	1031	1007	997
7500	$Gas - fraction$ [%]	39.5	33.8	32.2	29.4	27.7	26.5
	$Used - fraction$ [%]	68.7	82.0	85.8	92.2	96.3	99.1
	$CO_2 - avoid$ [t]	12278	13435	13760	14328	14673	14917
	€/$CO_2 - avoid$ [€/t]	961	878	858	824	804	791
10000	$Gas - fraction$ [%]	44.0	40.9	39.9	38.1	37.2	37.2
	$Used - fraction$ [%]	77.4	87.4	90.4	95.9	98.8	98.8
	$CO_2 - avoid$ [t]	15154	15992	16263	16750	16994	16994
	€/$CO_2 - avoid$ [€/t]	779	738	726	704	694	694
25000	$Gas - fraction$ [%]	56.4	56.2	56.1	56.1	56.1	56.1
	$Used - fraction$ [%]	97.2	99.3	99.4	99.4	99.4	99.4
	$CO_2 - avoid$ [t]	29495	29631	29698	29698	29698	29698
	€/$CO_2 - avoid$ [€/t]	400	398	397	397	397	397
50000	$Gas - fraction$ [%]	62.5	62.5	62.5	62.5	62.5	62.5
	$Used - fraction$ [%]	100	100	100	100	100	100
	$CO_2 - avoid$ [t]	50735	50735	50735	50735	50735	50735
	€/$CO_2 - avoid$ [€/t]	233	233	233	233	233	233

Table 6.6: Influence of thermal storage scenario 1

# Houses		Scenario 2					
	Storage size [m^3]	0	250	500	2000	5000	∞
1000	$Gas-fraction$ [%]	0	0	0	0	0	0
	$Used-fraction$ [%]	9.5	9.5	9.5	9.5	9.5	9.5
	$CO_2-avoid$ [t]	2726	2726	2726	2726	2726	2726
	€/$CO_2-avoid$ [€/t]	4329	4329	4329	4329	4329	4329
V-N	$Gas-fraction$ [%]	0	0	0	0	0	0
	$Used-fraction$ [%]	22.5	22.5	22.5	22.5	22.5	22.5
	$CO_2-avoid$ [t]	6466	6466	6466	6466	6466	6466
	€/$CO_2-avoid$ [€/t]	1825	1825	1825	1825	1825	1825
5000	$Gas-fraction$ [%]	4.3	1.5	1.1	0.3	0	0
	$Used-fraction$ [%]	44.5	46.4	46.6	47.2	47.4	47.4
	$CO_2-avoid$ [t]	13043	13425	13479	13588	13629	13629
	€/$CO_2-avoid$ [€/t]	905	879	875	868	866	866
7500	$Gas-fraction$ [%]	11.1	7.0	6.4	5.8	4.9	4.9
	$Used-fraction$ [%]	59.7	63.9	64.5	65.1	66.1	66.1
	$CO_2-avoid$ [t]	18174	19012	19135	19258	19442	19442
	€/$CO_2-avoid$ [€/t]	649	621	617	613	607	607
10000	$Gas-fraction$ [%]	17.6	14.5	14.2	13.7	12.9	9.8
	$Used-fraction$ [%]	70.6	74.9	75.3	76.0	77.1	81.4
	$CO_2-avoid$ [t]	22461	23306	23387	23524	23742	24587
	€/$CO_2-avoid$ [€/t]	525	506	505	502	497	480
25000	$Gas-fraction$ [%]	40.7	40.1	40.0	40.0	40.0	40.0
	$Used-fraction$ [%]	96.9	99.1	99.4	100	100	100
	$CO_2-avoid$ [t]	40409	40819	40887	40887	40887	40887
	€/$CO_2-avoid$ [€/t]	292	289	289	289	289	289
50000	$Gas-fraction$ [%]	54.4	54.4	54.4	54.4	54.4	54.4
	$Used-fraction$ [%]	100	100	100	100	100	100
	$CO_2-avoid$ [t]	62148	62148	62148	62148	62148	62148
	€/$CO_2-avoid$ [€/t]	190	190	190	190	190	190

Table 6.7: Influence of thermal storage scenario 2

# Houses		Scenario 3					
	Storage size [m^3]	0	250	500	2000	5000	∞
1000	$Gas-fraction$ [%]	9.10	1.5	0.9	0	0	0
	$Used-fraction$ [%]	9.48	11.4	11.6	11.8	11.8	11.8
	$CO_2-avoid$ [t]	2478	2685	2701	2726	2726	2726
	€/$CO_2-avoid$ [€/t]	3592	3315	3295	3265	3265	3265
V-N	$Gas-fraction$ [%]	12.8	3.5	2.2	0.5	0	0
	$Used-fraction$ [%]	20.3	25.9	26.7	27.7	28.0	28.0
	$CO_2-avoid$ [t]	5638	6239	6323	6433	6466	6466
	€/$CO_2-avoid$ [€/t]	1579	1426	1407	1383	1377	1377
5000	$Gas-fraction$ [%]	17.2	9.20	6.1	2.1	1.1	1.1
	$Used-fraction$ [%]	37.1	47.3	51.2	56.4	57.7	57.7
	$CO_2-avoid$ [t]	11285	12375	12798	13343	13479	13479
	€/$CO_2-avoid$ [€/t]	789	719	695	667	660	660
7500	$Gas-fraction$ [%]	20.1	13.7	11.1	6.0	4.6	4.6
	$Used-fraction$ [%]	50.1	62.4	67.3	77.1	79.7	79.7
	$CO_2-avoid$ [t]	16334	17643	18174	19217	19503	19503
	€/$CO_2-avoid$ [€/t]	545	504	490	463	456	456
10000	$Gas-fraction$ [%]	22.5	17.5	15.8	12.6	11.5	11.5
	$Used-fraction$ [%]	60.4	73.4	77.8	86.0	88.7	88.7
	$CO_2-avoid$ [t]	21124	22488	22951	23823	24123	24123
	€/$CO_2-avoid$ [€/t]	421	396	388	374	369	369
25000	$Gas-fraction$ [%]	32.4	31.5	31.2	30.7	30.7	30.7
	$Used-fraction$ [%]	88.0	93.8	95.8	99.1	99.1	99.1
	$CO_2-avoid$ [t]	46066	46679	46884	47224	47224	47224
	€/$CO_2-avoid$ [€/t]	193	191	190	188	188	188
50000	$Gas-fraction$ [%]	38.5	38.4	38.4	38.4	38.4	38.4
	$Used-fraction$ [%]	98.7	99.6	99.6	99.6	99.6	99.6
	$CO_2-avoid$ [t]	83818	83954	83954	83954	83954	83954
	€/$CO_2-avoid$ [€/t]	106	106	106	106	106	106

Table 6.8: Influence of thermal storage scenario 3

# Houses		Scenario 4					
	Storage size [m^3]	0	250	500	2000	5000	∞
1000	$Gas-fraction$ [%]	0	0	0	0	0	0
	$Used-fraction$ [%]	5.4	5.4	5.4	5.4	5.4	5.4
	$CO_2-avoid$ [t]	2726	2726	2726	2726	2726	2726
	€/$CO_2-avoid$ [€/t]	3265	3265	3265	3265	3265	3265
V-N	$Gas-fraction$ [%]	0	0	0	0	0	0
	$Used-fraction$ [%]	12.8	12.8	12.8	12.8	12.8	12.8
	$CO_2-avoid$ [t]	6466	6466	6466	6466	6466	6466
	€/$CO_2-avoid$ [€/t]	1377	1377	1377	1377	1377	1377
5000	$Gas-fraction$ [%]	0.5	0	0	0	0	0
	$Used-fraction$ [%]	26.9	26.9	26.9	26.9	26.9	26.9
	$CO_2-avoid$ [t]	13561	13629	13629	13629	13629	13629
	€/$CO_2-avoid$ [€/t]	656	653	653	653	653	653
7500	$Gas-fraction$ [%]	2.3	0.3	0.2	0	0	0
	$Used-fraction$ [%]	39.4	40.1	40.2	40.4	40.4	40.4
	$CO_2-avoid$ [t]	19973	20382	20403	20444	20444	20444
	€/$CO_2-avoid$ [€/t]	446	437	436	435	435	435
10000	$Gas-fraction$ [%]	4.7	1.7	1.4	0.7	0.7	0.7
	$Used-fraction$ [%]	49.6	51.8	52.1	53.0	53.0	53.0
	$CO_2-avoid$ [t]	25977	26975	26876	27067	27067	27067
	€/$CO_2-avoid$ [€/t]	343	332	331	329	329	329
25000	$Gas-fraction$ [%]	18.2	16.7	16.7	16.5	16.5	16.2
	$Used-fraction$ [%]	83.5	85.8	86.0	86.5	87.4	99.6
	$CO_2-avoid$ [t]	55743	56765	56765	56901	56901	57106
	€/$CO_2-avoid$ [€/t]	160	157	157	156	156	156
50000	$Gas-fraction$ [%]	29.7	29.1	29.1	29.1	29.1	29.1
	$Used-fraction$ [%]	99.6	99.6	99.6	99.6	99.6	99.6
	$CO_2-avoid$ [t]	95812	96630	96630	96630	96630	96630
	€/$CO_2-avoid$ [€/t]	93	92	92	92	92	92

Table 6.9: Influence of thermal storage scenario 4

7

Conclusions & recommendations

In this chapter, the conclusions of this research are presented by answering the research questions and recommendations for future research are discussed.

7.1. Conclusions

The main objective of the research was to gain insight into the possibility of extracting and utilising the thermal energy that is generated while producing hydrogen flexibly based on a wind profile using alkaline electrolysis. To do so, a case study based on the H2ermes project has been conducted, which assesses this feasibility using a newly constructed thermodynamic model and for four different scenarios. For every scenario a process flow diagram is designed using a pinch analysis, after which the design is analysed using the constructed model. Based on the results from the model the different sub questions can be answered and ultimately the main research question:

How can the heat generated in an alkaline water electrolysis plant, operated flexibly based on a wind power electricity pattern, be extracted from the process and applied in a district heating network?

Several sub questions that help answer the main research question are defined:The sub questions were defined as follows:

1. *How much thermal energy can or needs to be extracted from the process?*
2. *At what quality (temperature) can the heat extracted from the process?*
3. *How can the demand temperature of the chosen application be reached?*
4. *How does the efficiency of the system increase when the thermal energy is extracted?*
5. *How can the supply and the demand be balanced?*
6. *How does the application of the extracted thermal energy influence CO_2 emissions?*
7. *What would be the cost of adding a thermal extraction and utilisation system?*

To gain insight in the sub questions and ultimately the main research question, multiple criteria were investigated for the different scenarios as discussed in the results section (**??**). In order to answer the main research question, conclusions for the sub questions are discussed in the next paragraphs based on the outcome of the investigated criteria.

How much thermal energy can or needs to be extracted from the process?
The total amount of thermal energy that can be recovered from the process ($Recov - fraction$), with (scenario 1 and 2) or without (scenario 3 and 4) heat pump, depends on the age of the hydrogen production plant and on the capacity (inputted power). For scenario 3 and 4 the demand temperature (70^oC) is lower than the temperature of the electrolyser (80^oC) which results in the possibility to directly extract the thermal energy without having to be upgraded by a heat pump. Adding the thermal system shown in figure 6.3 for scenario 3 and 4 could extract 90%, 93.6% and up to 94.8% for start, middle

and and of life respectively when operating at full capacity. This relates to 18, 23 and 29 MW of thermal energy recovered. On average percentage that can be extracted is 84.9%, 91.3% and 92.4% for start, middle and end of life (on average means the average extracted percentage over all power inputs).

For scenario 1 and 2 the recovered thermal energy is the sum of the thermal energy recovered directly plus the thermal energy recovered by making use of a heat pump. Adding the thermal system shown in figure 5.5 could extract 62.9%, 78.9% and up to 89.2% for start, middle and and of life respectively when operating at full capacity. This relates to 13, 20 and 27 MW of thermal energy recovered. On average the percentage that can be extracted is 33.5%, 58% and 75.7% for start, middle and end of life.

It can be concluded that when the demand temperature is lower than the temperature in the electrolyser more energy can be recovered from the system than when it is the other way around. The difference between the average $Recov - fraction$ between scenario 3 and 4 and the results for 1 and 2 is 51.4%, 33.3%, 16.7% for start, middle and end of life respectively. However, the difference decreases as the capacity increases.

At what quality (temperature) can the heat extracted from the process?
The quality of the thermal energy largely depends on the operating temperature of the electrolyser since the flows leaving the electrolyser will have the same temperature. For this research a temperature of 80^{o}C was assumed. To upgrade the temperature above the temperature in the electrolyser the thermal energy that can be extracted in between the compressors needs to be used as the hydrogen/water vapor mixture is compressed to a temperature of 130^{o}C. But since only a small amount of thermal energy is available at these locations, this would result in a negligible amount of district heating water that could reach 85^{o}C. It can be concluded that when temperatures above the electrolyser temperature are demanded (scenario 1 and 2) another technique needs to be used to upgrade the quality.

How can the demand temperature of the chosen application be reached?
For scenario 3 and 4 the demand temperature can be reached by extracting the thermal energy directly as shown in the PFD (figure 6.3). For improving the quality of the thermal energy and for scenario 1 and 2 the implementation of a vapor compression heat pump was analysed. The use of a heat pump drastically increases the amount of thermal energy that can be extracted when the demand temperature is 85^{o}C. At full capacity, the increase is 13.2%, 21.2% and 24.8% for start, middle and end of life (see tables 6.3, 6.5 and 6.4). The external power (P_{ext}, compressor power) needed for these increases is 1.42, 2.27 and 3.12 MW. This of course has a large influence on the overall efficiency (η_{tot}), which is discussed in the next paragraph.

How does the efficiency of the system increase when the thermal energy is extracted? Without adding a thermal extraction system the overall efficiency would be the same as the efficiency of the electrolyser η_{elec}. The electrolyser efficiency decreases as the hydrogen plant ages as well as when the capacity increases. A efficiency of 91.2% could be reached when the plant operates at 25% at the start of its life, which decreases to 81% at the end of life. At the middle of life, when the plant operates at full capacity, an efficiency of 76.2% is found (see tables 6.3, 6.5 and 6.4). The electrolyser efficiencies are the same for all scenarios as no variations of electrolyser parameters are reviewed.

Adding the thermal extraction system increases the overall system efficiency (η_{tot}). This increase does differ per scenario as it is dependent on the thermal extraction system. For scenario 1 and 2, the efficiency increases with 11%, 16.8% and 21.8% for start, middle and end of life respectively at maximum capacity ($\eta_{tot} - \eta_{elec}$). For scenario 3 and 4, the efficiency increases with 17.6%, 23% and 25.7% for start, middle and end of life at maximum capacity. It can be concluded that the overall efficiency does indeed increase by adding the thermal extraction system and that the increase is higher for scenario 3 and 4 than for 1 and 2.

How can the supply and the demand be balanced?
For storing thermal energy multiple techniques are available. In this research the focus was on gaining insight in how much the addition of storage would benefit the overall system. In the previous paragraphs we looked at the overall efficiency (η_{tot}) assuming that all the extracted thermal energy was actually

used, but because of the difference in supply and demand this will not always be the case. The criteria indicating the percentage of extracted thermal energy actually used after addition of thermal storage is the $Used - fraction$ (tables 6.6, 6.7, 6.8 and 6.9) as a function of the number of houses within the district heating network and the storage size. From the results can be seen that for all scenarios a 100% used fraction can be reached when the amount of houses within the network increases: 25000, 25000, 50000 and 50000 houses for scenario 1, 2, 3 and 4 respectively. When this is the case, it can also be seen that the influence of the storage size is negligible.

For smaller heating districts, the size of thermal storage does influence the $Used - fraction$. For 5000 houses, adding 250 m^3 of thermal increases the fraction with 14.6%, 1.9%, 10.2% and 0% for scenario 1, 2, 3 and 4 respectively. For scenario 2 and 4 the influence of thermal storage is negligible since the baseload of 70% minimises the gap between supply in demand.

It can be concluded that adding thermal storage is not feasible when the size of the hating district surpasses 25000 houses and that for the baseload cases (scenario 2 and 4), adding thermal storage is not feasible at all. For scenario 1 and 3, adding thermal storage benefits the $Used - fraction$ when the district is below 25000 houses but only up to a certain size.

How does the application of the extracted thermal energy influence CO_2 emissions?
Using the thermal energy from the hydrogen production plant results in a reduction in the use of natural gas to provide the houses in the heating district with thermal energy. tables 6.6, 6.7, 6.8 and 6.9 show the $Gas - fraction$ (percentage of normal yearly gas use still needed). This value is also expressed in the amount of CO_2 avoided ($CO_2 - avoid$). As the $Gas - faction$ decreases, the $CO_2 - avoid$ increases.

One household emits on average 7.5 tonnes of CO_2 per year directly (energy in house plus transportation). When dividing the $CO_2 - avoid$ by the number of houses the avoided CO_2 per house can be calculated as shown in tables 7.1 and 7.2.

	Scenario 1						Scenario 2					
# Houses	$CO_2 - avoid/house$ [t]						$CO_2 - avoid/house$ [t]					
Storage size [m^3]	0	250	500	2000	5000	∞	0	250	500	2000	5000	∞
1000	2.21	2.64	2.65	2.71	2.71	2.71	2.48	2.68	2.70	2.73	2.73	2.73
V-N	2.00	2.41	2.53	2.65	2.71	2.71	2.38	2.63	2.67	2.71	2.73	2.73
5000	1.79	2.04	2.13	2.29	2.34	2.37	2.26	2.48	2.56	2.67	2.70	2.70
7500	1.64	1.79	1.83	1.91	1.96	1.99	2.18	2.35	2.42	2.56	2.60	2.60
10000	1.52	1.60	1.63	1.68	1.70	1.70	2.11	2.25	2.30	2.38	2.41	2.41
25000	1.18	1.19	1.19	1.19	1.19	1.19	1.84	1.87	1.88	1.89	1.89	1.89
50000	1.01	1.01	1.01	1.01	1.01	1.01	1.68	1.68	1.68	1.68	1.68	1.68

Table 7.1: CO_2 avoided per household for scenario 1 and 2

	Scenario 3						Scenario 4					
# Houses	$CO_2 - avoid/house$ [t]						$CO_2 - avoid/house$ [t]					
Storage size [m^3]	0	250	500	2000	5000	∞	0	250	500	2000	5000	∞
1000	2.73	2.73	2.73	2.73	2.73	2,73	2.73	2.73	2.73	2.73	2.73	2.73
V-N	2.73	2.73	2.73	2.73	2.73	2,73	2.73	2.73	2.73	2.73	2.73	2.73
5000	2.61	2.68	2.70	2.72	2.73	2,73	2.71	2.73	2.73	2.73	2.73	2.73
7500	2.42	2.53	2.55	2.57	2.59	2,59	2.66	2.72	2.72	2.73	2.73	2.73
10000	2.25	2.33	2.34	2.35	2.37	2,46	2.60	2.68	2.69	2.71	2.71	2.71
25000	1.62	1.63	1.64	1.64	1.64	1,64	2.23	2.27	2.27	2.28	2.28	2.28
50000	1.24	1.24	1.24	1.24	1.24	1,24	1.92	1.93	1.93	1.93	1.93	1.93

Table 7.2: CO_2 avoided per household for scenario 3 and 4

It can be concluded that the maximum avoided CO_2 is equal to 2.73 tonnes which is 36.4% of the average yearly household CO_2 emissions.

What would be the cost of adding a thermal extraction and utilisation system?
The investment necessary for the thermal system is mainly dependent on the cost for the piping from the plant to Velsen-Noord and the heat pump that may be used when improving the quality of the thermal energy is necessary. The plant side of the thermal system (heat exchangers) need a relatively low investment, which in part would also be made when thermal energy is not extracted but just cooled away. The investment cost for scenario 1 and 2 are the same, namely 11.8 million euros. The investment cost for scenario 3 and 4 are also the same, namely 8.9 million euros.

After accounting for the sub-research objectives, the main objective of this research can be assessed, which is formulated as follows:

How can the heat generated in an alkaline water electrolysis plant, operated flexibly based on a wind power electricity pattern, be extracted from the process and applied in a district heating network?

To answer the main research question a case study was conducted based on the H2ermes project and the application of the extracted thermal energy in Velsen-Noord. It can be concluded that when a baseload of 70% is maintained (scenario 2 and 4), the $Gas - fraction$ becomes 0%, which means that in theory, no gas would be necessary to provide thermal energy to the 2372 houses. However, for scenario 2 the $Used - fraction$ is 9.7% higher than for scenario 4 and the €$/CO - 2 - avoid$ is 448 euros higher for scenario 2 than for scenario 4. It can be concluded that adding thermal storage for Velsen-Noord and the baseload cases is not beneficial.

Since it is probable that the hydrogen plant will operate under a certain baseload and will not follow the wind profile entirely, the best solution for extracting the thermal energy would as described in scenario 4 since this solution would be cheaper and a value of 2.73 tonnes of CO_2 avoided per household could be managed. The extraction system would look like the PFD shown in figure **??**, but no thermal storage would be necessary.

7.2. Recommendations

The research provides insight in the possible extraction and utilisation of the generated thermal energy. The following recommendations are given for further studies:

For this study it was assumed (based on input from Nouryon) that the operational temperature of the electrolyser is equal to 80^{o}C. For further study it could be very interesting to investigate the influence of electrolyzer operational temperatures. Both higher (other alkaline technologies) and lower (PEM technologies).

Increasing the pressure in the electrolyser and this in the separators will decrease the amount of water vapor on both the cathode and anode side. Modelling the proposed systems for different electrolyser pressures would give more insight into the system. Of course increasing the pressure will result into other technological challenges which would also need to be researched. Increasing the pressure will mean that more thermal energy can be extracted from the flow back to the electrolyser and a smaller flow from the separators to the condensers.

In the model thermal losses in all the different components are not taken into account. Losses in piping, radiation form the electrolyser, radiation form heat exchangers and losses during thermal storage. For further detailed study it these losses should be taken into account to get a better representation of the available thermal energy that can be extracted. These losses will probably only be a small fraction from the total amount of thermal energy generated, but it would provide more insight into the system if analysed.

For modelling the demand form the heating district a dataset provided by HVC was used. There are, however, methods for the detailed modelling of a district based on the sort of real estate, outside temperature and gas use. The dataset used for this study gives an estimate for the demand, but when a

more accurate and district specific demand profile is modelled the outcome of the model will also give a better representation of the amount of houses that could be supplied with thermal energy.

For the application of thermal energy a heating district was chosen since this was relevant for the H2ermes project. Since hydrogen is on the rise which also means that the number of hydrogen production plants all over the world will increase, it would also be relevant to research which other applications could be found for low grade energy generated during alkaline electrolysis. Examples could be power form low grade thermal energy or technologies where low grade thermal energy is used to provide cooling.

For now a baseload of 70% was chosen to be investigated. It is also relevant to investigate other baseload cases and do a feasibility study that takes the produced amount of hydrogen into account in relation to the avoided amount of gas within the district heating system. To do this, a further study into the economics of the system has to be conducted. As for now, only a study into the investment cost was done. To draw conclusions about whether higher hydrogen production or more avoided gas use is beneficial, the cost and gains for hydrogen and providing thermal energy need to be evaluated. This can only be done when the levelized cost of energy (LCoE) is known. For this the operational cost, lifetimes and investment costs of the different components of the system need to be taken into account.
For future study it would also be interesting to review how the amount of euros per CO_2 avoided can be minimised. Would other electrolyser technologies be more beneficial or other operating points in terms of pressure and temperature in the alkaline electrolyser?

References

[1] Z. Abdin, C.J. Webb, and E.MacA. Gray. “Modelling and simulation of an alkaline electrolyser cell”. In: *Energy* 138 (2017), pp. 316–331. ISSN: 0360-5442. DOI: https://doi.org/10.1016/j.energy.2017.07.053. URL: http://www.sciencedirect.com/science/article/pii/S0360544217312288.

[2] Alfalaval. *5 Reasons to use plate-and-frame heat exchangers instead of shell-and-tube*. URL: https://www.alfalaval.com/microsites/gphe/tools/gphe-vs-shell-and-tube/.

[3] Port of Amsterdam. *Nouryon, Tata Steel en Port of Amsterdam werken samen aan project H2ermes: groene waterstof voor de regio Amsterdam*. URL: https://www.portofamsterdam.com/nl/nieuws/h2ermes-groene-waterstof.

[4] Carlos A. Infante Ferreira Anton A. Kiss. *HEat pumps in chemical process industry*. CRC Press, 2017.

[5] Opeyemi Bamigbetan et al. “Review of vapour compression heat pumps for high temperature heating using natural working fluids”. In: *International Journal of Refrigeration* 80 (2017), pp. 197–211. ISSN: 0140-7007. DOI: https://doi.org/10.1016/j.ijrefrig.2017.04.021. URL: https://www.sciencedirect.com/science/article/pii/S0140700717301780.

[6] Dmitri Bessarabov and Pierre Millet. “Chapter 3 - Fundamentals of Water Electrolysis”. In: *PEM Water Electrolysis*. Ed. by Dmitri Bessarabov and Pierre Millet. Hydrogen Energy and Fuel Cells Primers. Academic Press, 2018, pp. 43–73. ISBN: 978-0-12-811145-1. DOI: https://doi.org/10.1016/B978-0-12-811145-1.00003-4. URL: http://www.sciencedirect.com/science/article/pii/B9780128111451000034.

[7] Christophe Coutanceau, Stève Baranton, and Thomas Audichon. “Chapter 3 - Hydrogen Production From Water Electrolysis”. In: *Hydrogen Electrochemical Production*. Ed. by Christophe Coutanceau, Stève Baranton, and Thomas Audichon. Hydrogen Energy and Fuel Cells Primers. Academic Press, 2018, pp. 17–62. ISBN: 978-0-12-811250-2. DOI: https://doi.org/10.1016/B978-0-12-811250-2.00003-0. URL: http://www.sciencedirect.com/science/article/pii/B9780128112502000030.

[8] csidesigns. *TOP 7 REASONS TO PURCHASE A PLATE-AND-FRAME INSTEAD OF A SHELL-AND-TUBE HEAT EXCHANGER*. URL: https://www.csidesigns.com/blog/articles/shell-and-tube-heat-exchanger-why-purchase-plate-and-frame.

[9] Abdulrahman Dahash et al. “Advances in seasonal thermal energy storage for solar district heating applications: A critical review on large-scale hot-water tank and pit thermal energy storage systems”. In: *Applied Energy* 239 (2019), pp. 296–315. ISSN: 0306-2619. DOI: https://doi.org/10.1016/j.apenergy.2019.01.189. URL: https://www.sciencedirect.com/science/article/pii/S0306261919301837.

[10] Energy.gov. *Hydrogen Production: Natural Gas Reforming*. URL: https://www.energy.gov/eere/fuelcells/hydrogen-production-natural-gas-reforming#:~:text=In%20steam%2Dmethane%20reforming%2C%20methane,for%20the%20reaction%20to%20proceed..

[11] Hydrogen Europe. *Hydrogen Production*. URL: https://hydrogeneurope.eu/hydrogen-production-0.

[12] Walter Grassi. *Heat pumps: Fundamentals and Applications*. Springer, 2018.

[13] IEA. “The future of hydrogen: Seizing today’s oppotunities”. In: (2019).

[14] IRENA. “Global Energy Transformation: A roadmap to 2050”. In: (2018).

[15] IRENA. “Reaching zero with renewables”. In: (2020).

[16] Anton A. Kiss and Carlos A. Infante Ferreira. *Heat pumps in chemical process industry*. CRC Press, Taylor and Francis Group, 2017.

[17] B. Linnhoff and E. Hindmarsh. “The pinch design method for heat exchanger networks”. In: *Chemical Engineering Science* 38.5 (1983), pp. 745–763. ISSN: 0009-2509. DOI: https://doi.org/10.1016/0009-2509(83)80185-7. URL: https://www.sciencedirect.com/science/article/pii/0009250983801857.

[18] Charles Maxwell. *Cost Indices*. URL: https://www.toweringskills.com/financial-analysis/cost-indices/.

[19] Pierre Millet and Sergey Grigoriev. “Chapter 2 - Water Electrolysis Technologies”. In: (2013). Ed. by Luis M. Gandía, Gurutze Arzamendi, and Pedro M. Diéguez, pp. 19–41. DOI: https://doi.org/10.1016/B978-0-444-56352-1.00002-7. URL: https://www.sciencedirect.com/science/article/pii/B9780444563521000027.

[20] Henrik Pieper et al. “Allocation of investment costs for large-scale heat pumps supplying district heating”. In: *Energy Procedia* 147 (2018). International Scientific Conference “Environmental and Climate Technologies”, CONECT 2018, 16-18 May 2018, Riga, Latvia, pp. 358–367. ISSN: 1876-6102. DOI: https://doi.org/10.1016/j.egypro.2018.07.104. URL: https://www.sciencedirect.com/science/article/pii/S1876610218302613.

[21] A.J. Sangster. “Engineering the early demise of fossil fuels”. In: *International Journal of Sustainable and Green Energy* 3 (Jan. 2015), pp. 115–122. DOI: 10.11648/j.ijrse.20140306.11.

[22] Mangold Schmidt Thomas. *Large-scale heat storage*. CRC Press, 2017.

[23] Ray Sinnott and Gavin Towler. “Chapter 1 - Introduction to Design”. In: *Chemical Engineering Design (Sixth Edition)*. Ed. by Ray Sinnott and Gavin Towler. Sixth Edition. Chemical Engineering Series. Butterworth-Heinemann, 2020, pp. 1–45. ISBN: 978-0-08-102599-4. DOI: https://doi.org/10.1016/B978-0-08-102599-4.00001-1. URL: https://www.sciencedirect.com/science/article/pii/B9780081025994000011.

[24] Ray Sinnott and Gavin Towler. “Chapter 6 - Costing and Project Evaluation”. In: *Chemical Engineering Design (Sixth Edition)*. Ed. by Ray Sinnott and Gavin Towler. Sixth Edition. Chemical Engineering Series. Butterworth-Heinemann, 2020, pp. 275–369. ISBN: 978-0-08-102599-4. DOI: https://doi.org/10.1016/B978-0-08-102599-4.00006-0. URL: https://www.sciencedirect.com/science/article/pii/B9780081025994000060.

[25] Tobias Sommer et al. “The reservoir network: A new network topology for district heating and cooling”. In: *Energy* 199 (2020), p. 117418. ISSN: 0360-5442. DOI: https://doi.org/10.1016/j.energy.2020.117418. URL: https://www.sciencedirect.com/science/article/pii/S0360544220305259.

[26] UNFCCC. *What is the Paris agreement?* URL: https://unfccc.int/process-and-meetings/the-paris-agreement/what-is-the-paris-agreement.

[27] Celsius Wiki. *Thermal Energy Storage*. 2020. URL: https://celsiuscity.eu/thermal-energy-storage/?utm_source=rss&utm_medium=rss&utm_campaign=thermal-energy-storage.

[28] Kai Zeng and Dongke Zhang. “Recent progress in alkaline water electrolysis for hydrogen production and applications”. In: *Progress in Energy and Combustion Science* 36.3 (2010), pp. 307–326. ISSN: 0360-1285. DOI: https://doi.org/10.1016/j.pecs.2009.11.002. URL: http://www.sciencedirect.com/science/article/pii/S0360128509000598.

8

Task Division

Table 8.1: Distribution of the workload

	Task	Student Name(s)
	Summary	
Chapter 1	Introduction	
Chapter 2		
Chapter 3		
Chapter *		
Chapter *	Conclusion	
	Editors	
	CAD and Figures	
	Document Design and Layout	